Materials for excitons–polaritons: Exploiting the diversity of semiconductors

J. Bellessa, J. Bloch, E. Deleporte, V.M. Menon, H.S. Nguyen, H. Ohadi, S. Ravets, and T. Boulier*

The regime of strong coupling between photons and excitons gives rise to hybrid light–matter particles with fascinating properties and powerful implications for semiconductor quantum technologies. As the properties of excitons crucially depend on their host crystal, a rich field of exciton–polariton engineering opens by exploiting the diversity of semiconductors currently available. From dimensionality to binding energy to unusual orbitals, various materials provide different fundamental exciton properties that are often complementary, enabling vast engineering possibilities. This article aims to showcase some of the main materials for strong light–matter engineering, focusing on their fundamental complementarity and what this entails for future quantum technologies.

Introduction

In todays large field of semiconductor physics, the control over light–matter coupling has spawned a captivating object: the exciton–polariton. These hybrid light–matter quasiparticles emerge from the admixture between excitons (bound electron–hole pairs) and photons. While exciton–polaritons exist in bulk semiconductors, major advances have been obtained with two-dimensional (2D) excitons confined in an heterostructure (e.g., a quantum well) embedded within an optical microcavity,[1] as represented in **Figure 1**a. Exciton–polaritons possess a unique blend of properties inherited from both their excitonic part and their photonic part, making them a subject of intense research interest with implications ranging from fundamental physics[2] to practical applications in optoelectronics[3] and quantum technologies.[4]

At its core, exciton–polariton research revolves around manipulating their properties to engineer specific systems of interest. The properties of an exciton–polariton gas arise from the delicate balance between the exciton–photon coupling, the exciton–exciton interactions, and the various interactions with the semiconductor environment (phonons, exciton band structure, crystal (an)isotropy, incoherent exciton reservoir,...). The exciton–photon coupling strength, g, is usually controlled via the choice of material and the optical microcavity design: its quality factor, mode volume, and dimensionality all contribute to shaping exciton–polaritons. The interactions between two excitons are typically set by the wavefunction size and shape, itself governed by the choice of semiconductor material. One of the most striking features of exciton–polaritons is their non-parabolic dispersion relation, displayed in Figure 1b, which is partly responsible for their peculiar properties, such as a momentum-dependent effective mass and photon–exciton mixing ratio.

This dispersion relation arises from the diagonalization of the Hamiltonian describing the coupled exciton–photon system within the microcavity:

$$\hat{H} = \begin{pmatrix} E_X - i\frac{\hbar}{2}\gamma_X & g \\ g & E_C - i\frac{\hbar}{2}\kappa \end{pmatrix},$$

J. Bellessa, Université Lyon, Université Claude Bernard Lyon 1, CNRS, Institut Lumière Matière, 69622 Lyon, France; joel.bellessa@univ-lyon1.fr

J. Bloch, Centre de Nanosciences et de Nanotechnologies, CNRS, Université Paris-Sud, Université Paris-Saclay, 91120 Palaiseau, France; jacqueline.bloch@c2n.upsaclay.fr

E. Deleporte, Université Paris-Saclay, ENS Paris-Saclay, CentraleSupélec, Lumière, Matière et Interfaces (LuMIn) Laboratory, 91190 Gif-sur-Yvette, France; emmanuelle.deleporte@ens-paris-saclay.fr

V.M. Menon, Department of Physics, City College of New York, New York, NY, USA; Department of Physics, The Graduate Center, City University of New York, New York, NY, USA; vmenon@ccny.cuny.edu

H.S. Nguyen, Université Lyon, Ecole Centrale de Lyon, INSA Lyon, Université Claude Bernard Lyon 1, CPE Lyon, CNRS, INL, UMR5270, 69130 Ecully, France; hai-son.nguyen@ec-lyon.fr
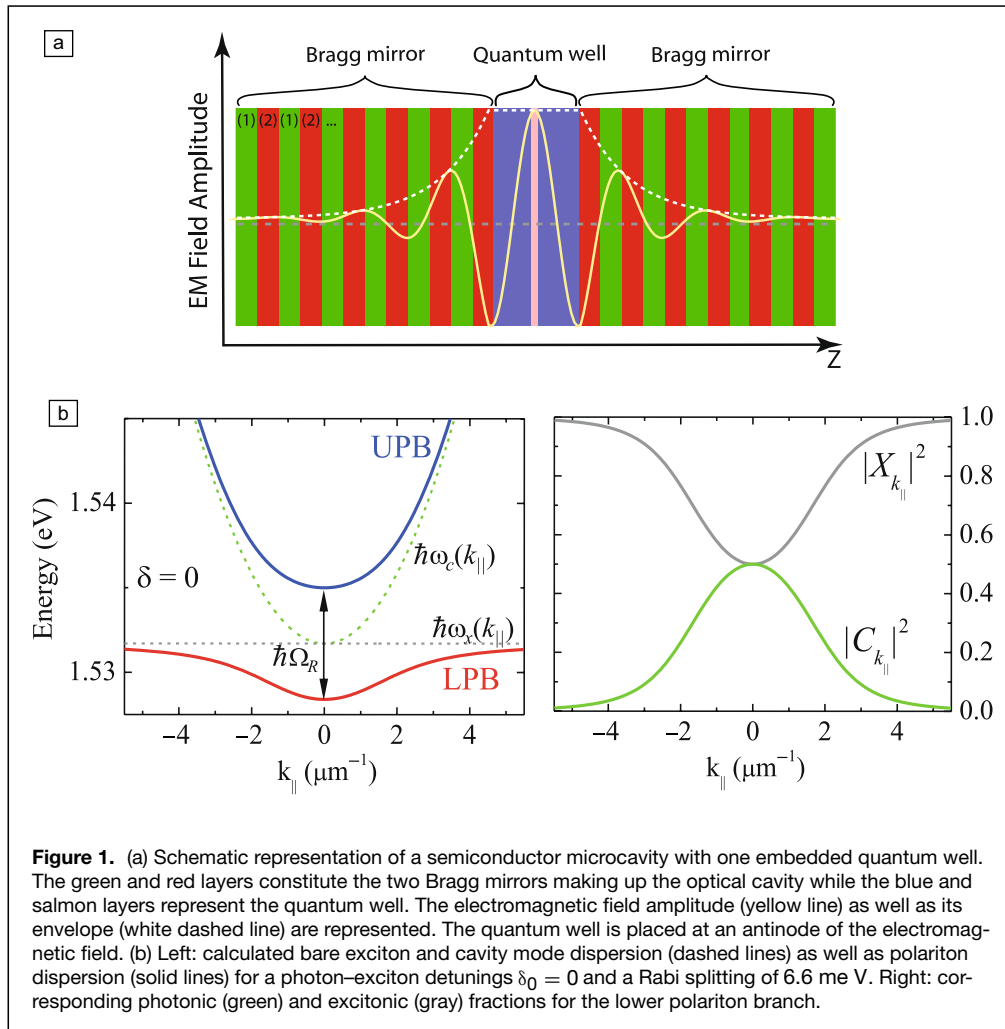
H. Ohadi, School of Physics and Astronomy, University of St Andrews, St Andrews KY16 9SS, UK; ho35@st-andrews.ac.uk

S. Ravets, Centre de Nanosciences et de Nanotechnologies, CNRS, Université Paris-Sud, Université Paris-Saclay, 91120 Palaiseau, France; sylvain.ravets@c2n.upsaclay.fr

T. Boulier, Université de Toulouse, INSA-CNRS-UPS, LPCNO, 135 Av. Rangueil, 31077 Toulouse, France; boulier@insa-toulouse.fr

*Corresponding author
doi:10.1557/s43577-024-00779-6

Figure 1. (a) Schematic representation of a semiconductor microcavity with one embedded quantum well. The green and red layers constitute the two Bragg mirrors making up the optical cavity while the blue and salmon layers represent the quantum well. The electromagnetic field amplitude (yellow line) as well as its envelope (white dashed line) are represented. The quantum well is placed at an antinode of the electromagnetic field. (b) Left: calculated bare exciton and cavity mode dispersion (dashed lines) as well as polariton dispersion (solid lines) for a photon–exciton detunings $\delta_0 = 0$ and a Rabi splitting of 6.6 me V. Right: corresponding photonic (green) and excitonic (gray) fractions for the lower polariton branch.

Experimentally, polaritons can be efficiently excited and read-out using optical spectroscopy techniques. On the one hand, so-called "nonresonant" excitation using a highly blue-detuned laser allows the incoherent pumping of polaritons followed, in some materials, by the emergence of a macroscopic phase through condensation processes. On the other hand, resonant excitation allows creating polariton fluids with well-chosen energy, phase, and amplitude. By monitoring photons leaking out of the cavity, polariton modes can be fully characterized as the phase and amplitude of their wavefunction can be imaged both in real and reciprocal spaces with (pseudo)spin resolution. Moreover, their statistics are directly accessible via the emitted photon statistics.

From a fundamental perspective, exciton–polaritons are one of the few systems that exhibit superfluidity,[5] Bose–Einstein condensation (BEC),[6] quantum vortices,[7] and solitons,[8] up to room temperature in some materials.[9] For example, superfluidity arises from both the long-range coherence issued by the photonic side and from the interaction effects issued by the excitonic side. While similar to other quantum fluids (e.g., superfluid helium or atomic condensates), exciton–polaritons add a twist: it is a (nonequilibrium) driven dissipative system, from which new behavior can emerge.[10] While a few optical systems (lasers, photorefractive systems, propagating nonlinear optics) exhibit some of these properties, exciton–polaritons possess some of the strongest nonlinearities, which makes them especially apt to mimic and complement cold atoms-based quantum fluids.[3,11]

Typically, the material can be spatially structured to suit a precise experimental scheme. For example, it can be designed to capture the essence of a more complex physical system, which is the principle of quantum simulation.[12] It can also be designed to boost certain aspects of exciton–polaritons, for example, their interaction to enhance interaction-induced quantum correlations.[13,14] This illustrates that

where E_X is the energy for the excitonic states, E_C is the energy for the cavity photon states, γ_X represents the decay rate of excitons, and κ the dissipation rate of photons due to cavity losses. The two eigenstates reveal two distinct dispersion relations: the upper polariton branch $E_+(\mathbf{k})$ (UPB) and the lower polariton branch (LPB) $E_-(\mathbf{k})$. The crux of engineering polariton is to ensure the strong coupling regime, whereby the dissipation rates γ_X and κ are much smaller than the coupling rate $g/\hbar$. In this limit, the dispersion relation becomes

$$E_\pm(\mathbf{k}) = \frac{1}{2}\left(E_X(\mathbf{k}) + E_C(\mathbf{k}) \pm \sqrt{\delta_\mathbf{k}^2 + \hbar^2\Omega_R^2} \right), \quad (1)$$

where $E_X(\mathbf{k})$ is the dispersion relation of bare excitons and $E_C(\mathbf{k})$ denotes the dispersion relation of photons in the cavity plane. Here, $\hbar\Omega_R = \sqrt{4g^2 - \hbar^2(\gamma_X + \kappa)^2} \sim 2g$ is the energy associated to the Rabi pulsation Ω_R and $\delta_\mathbf{k} = (E_X(\mathbf{k}) - E_C(\mathbf{k}))$ is the exciton–photon energy detuning at the momentum $\hbar\mathbf{k}$. This dispersion exhibits an anticrossing behavior between the exciton and photon modes, a hallmark of the strong light–matter coupling responsible for their admixture.

exciton–polaritons represent a rich playground for probing fundamental physics and studying novel quantum states of matter, with insights into quantum hydrodynamics, condensed-matter physics, and nonlinear optics.

On the practical side, exciton–polaritons have garnered significant interest for their potential applications in opto-electronic devices[15] and quantum technologies.[16] Due to their strong light–matter interaction and the ability to propagate over long distances within (one-dimensional [1D] and 2D) microcavities, exciton–polaritons can be utilized for the development of efficient light sources,[17] low-threshold lasers,[18] and integrated photonic circuits.[15] Moreover, their unique nonlinear optical properties and large spatial coherence make them promising candidates for applications in quantum information processing, where the coherent manipulation and the (nonlinear) control of quantum states are essential.[16]

In this scientific landscape, exploiting the diversity of semiconductors becomes judicious for several reasons. First, different semiconductor materials offer distinct electronic and optical properties for excitons such as bandgap energy, binding energy, and exciton–photon coupling strength. By selecting appropriate semiconductor materials, the properties of exciton–polaritons (e.g., their effective mass) can be tailored to suit specific applications (e.g., UV light-emitting diodes with ZnO[19]), to explore particular physical phenomena (e.g., room-temperature condensation with perovskites[20]) or even to provide them with new properties (e.g., valley degree of freedom in TMD monolayers[21]). Second, leveraging the diversity of semiconductors enables the exploration of novel material platforms and the enhancement of device performance (coherence, stability, nonlinear properties of exciton–polariton-based devices). Finally, the diversity of semiconductors could facilitate the integration of exciton–polaritons with existing semiconductor technologies, paving the way for seamless integration into practical devices and systems. As different semiconductors offer distinct advantages and challenges, the exploration and selection of materials is critical in shaping the future of exciton–polariton research.

In this article, we will delve into the diverse landscape of semiconductor materials utilized in the study of exciton–polaritons, examining their respective merits and limitations. By exploring the interplay between the choice of semiconductor material and exciton–polariton physics, we aim to provide a comprehensive overview of the current state-of-the-art in this rapidly evolving field.

Exciton–polaritons in epitaxially grown materials

Cavity polaritons were evidenced for the first time in 1992 using a GaAs-based microcavity.[22] At that time, GaAs was the material of choice, optimized for optoelectronics applications and benefiting from more than a decade of experimental developments in epitaxial techniques. One key advantage of these materials is the very small lattice mismatch between AlAs and GaAs crystals offering the possibility of growing high reflectivity Bragg mirrors using $Al_xGa_{1-x}As$ alloys. This has led to the emergence of high finesse ($10^3 \sim 10^4$) Fabry–Perot microcavities and of highly controlled cavity devices such as Surface Emitting Lasers (VCSELs) operating at room temperature both with electrical or optical injection. Moreover, when moving to cryogenic temperatures (below 10 K) the great material purity provides very narrow exciton linewidths. The exciton energy can also be tuned by selecting the proper alloy. These excellent properties, combined with the availability of well-developed technological tools, make them ideal for the studying fundamental physics. Thus, the field of quantum fluids of light (polariton gases[1]) emerged using the GaAs platform. This platform is also advantageous for the demonstration of innovative proofs of principle for photonic devices based on polaritonic effects.[23] Note that other epitaxially grown materials were also available in the early 2000s such as II–VI alloys (CdTe) and GaN quantum wells. Despite the fact that their growth was less controlled, leading to stronger disorder effects, these materials also played an important role in the development of the field.

Cavity polaritons being hybrid exciton–photon quasiparticles, their photonic part provides them with a low effective mass $\sim 10^{-5}m_e$ enabling BEC at elevated temperatures. Moreover, these effective masses can be made different for TE and TM polarizations, leading to an effective spin–orbit coupling for photons.[24] Because of the constant cavity photons leakage, polaritons are driven dissipative in nature and implement non-equilibrium physics. The excitonic component provides polarization-dependent Kerr nonlinearities through exciton–exciton interactions that are at the heart of the physics of quantum fluids of light.[1] Additionally, cavity polaritons also show strong magneto-optics response following the Zeeman splitting of excitons under a magnetic field. Finally, the excitons provide the gain material for polariton condensation or photon lasing.

Under resonant pumping, nonlinear parametric processes (optical parametric oscillation [OPO] and amplification [OPA]) were demonstrated in 2000 when exciting the system at the inflexion point of the lower polariton branch: signal and idler beams were clearly resolved.[25] A few years later, optical bistability was reported in GaAs cavities by monitoring the transmission intensity under resonant excitation.[26] Based on such degenerate four-wave mixing, squeezing below the standard quantum limit could then be measured.[27]

Another landmark was the demonstration of BEC of polaritons under nonresonant pumping. This manifests by the macroscopic population of a given polariton state via bosonic stimulation and the emergence of extended coherence through U(1) symmetry breaking of the phase. Polariton condensation was first demonstrated in CdTe based cavities (II–VI materials) because of efficient polariton scattering.[6] The resulting condensate profile was highly inhomogeneous because of disorder-induced localization. In GaAs-based structures, a relaxation bottleneck had to be overcome to reach condensation while maintaining the strong coupling regime.[28] This

could be achieved via exciton exciton scattering in samples with 12 quantum wells.[29] In parallel, polariton lasing was achieved at room temperature in GaN microcavities benefiting from the higher exciton binding energy preventing exciton ionization at high temperatures.[30] Importantly, polariton condensates exhibit distinct features from atomic condensates due to their out-of-equilibrium nature, as highlighted recently with the demonstration of Kardar Parisi Zhang universal scaling in the spatio-temporal coherence decay.[31]

Another striking result has been the prediction[32] and demonstration[5] of superfluidity of a resonantly driven polariton fluid. This is a direct consequence of the modification of the polariton–excitation spectrum induced by optical nonlinearities.[33] Other investigations of the hydrodynamical properties of polaritons have led to the observation of quantized vortices, solitons, half-vortices, and half-solitons.[1]

More recently, leveraging their tunability, polaritons have been used to study the physics of various Hamiltonians, in effect enabling polariton-based quantum simulators. For instance, the spin–orbit coupling term, which results in an effective magnetic field in reciprocal space, has been used to demonstrate the optical spin Hall effect.[34] In addition, in the presence of birefringence and time-reversal symmetry breaking, nonzero Berry curvature emerges, and the quantum geometric tensor was fully characterized.[35] The presence of gain, dissipation, and polarization-sensitive losses leads to nonhermitian physics, featuring, for example, exceptional points that are actively being studied in the context of non-hermitian topological photonics.[36] An important development has been the introduction of nanotechnology techniques to laterally confine polaritons.[37] Adjusting the confining potential allows engineering the band structure and emulating various Hamiltonians.[38] Lattices with phase frustration between sites could be implemented, featuring flatbands, where condensation, disorder-induced localization,[39] and exotic spin structures emerging in the presence of spin–orbit coupling[40] were explored. The exquisite control over the potential landscape also enabled realizing quasi-periodic lattices for polaritons. Gap labeling could be illustrated in Fibonacci structures,[41] and the emergence of criticality was carefully analyzed.[42] Realizing honeycomb lattices, Dirac physics have been explored with polaritons.[43] Emulating the effect of uniaxial strain, tilted and type III Dirac cones could be observed.[44] Adding spin–orbit coupling has led to the observation of spin-textures characteristic of the Dresselhaus spin–orbit interaction.[45] In the presence of time-reversal symmetry breaking, a polariton topological insulator was realized.[46]

In parallel to these fundamental investigations, proofs of principle for polariton devices were implemented. Over the years, various components have enriched the polariton device toolbox, such as interferometers, spin switches, optical transistors, ultrafast OPOs, polariton diodes,[23] and more recently, topological lasers,[47] and orbital microlasers.[48] Such devices have opened the way toward digital optical computing, with the hope of speeding up computation times.[23] Analog computing strategies are also being explored: for instance, coupled condensates were used as Ising machines,[49] and polariton nonlinearities enabled to demonstrate machine learning.[50]

The polariton platform with epitaxially grown materials presents such a degree of control that new research directions are currently emerging. Photonic systems have been highlighted as a great asset to explore topological physics beyond what is achieved with conservative systems.[51] In this sense, the polariton platform offers the ability to combine nonhermiticity, topology, drive, gain, and dissipation. For instance, the non-hermitian skin effect has been predicted in polariton lattices,[52] and new ways to define the quantum geometric tensor for non-hermitian polaritons are being proposed.[53] An exciting current challenge is to investigate topology in regimes where polariton nonlinearities become significant.[54,55] New methods are being developed to investigate Bogoliubov excitations on top of a nonlinear steady state,[33] where new topological features are expected.[56] Analog gravity can be emulated with polariton fluids,[2] and acoustic black holes have been realized by engineering an interface between subsonic and supersonic polariton flows.[57,58] Probing correlations between photons emitted on each side of the event horizon is expected to reveal the Hawking radiation.[59] Another exciting degree of freedom is provided by phonons residing in polariton microresonators so that new photon–exciton–phonon polaritons emerge, opening new avenues both for polaritonics and for optomechanics.[60–63] Finally, an exciting perspective is to make use of the quantum nature of polaritons that has been proposed to reach photon fermionization,[64] explore driven dissipative Bose-Hubbard physics,[65] and produce multiphoton entangled states. Quantum polaritonics is currently at its infancy, and first indications of the quantum nature of polaritons were observed recently through correlation measurements.[13,14,66] Various strategies are currently being investigated to increase polariton interactions and go deeper into the quantum regime, by developing new active materials featuring dipolar polaritons,[67] Fermi-polaron polaritons,[68,69] or by investigating new materials that are discussed in the following.

Exciton–polaritons in oxide semiconductors

In this section, we spotlight ZnO and Cu_2O as standout examples of oxides renowned for their well-documented excitonic properties, which are ideally suited for polaritonic applications. ZnO, a IIb–VI direct wide bandgap semiconductor with a room-temperature energy gap ($E_g \sim 3.4$ eV), is highlighted for its nontoxic, abundant, recyclable nature, and its compatibility with alloying processes involving MgO, BeO, and CdO.[73] Its excitons possess a substantial binding energy of ~60 meV, ensuring their stability at room temperature.
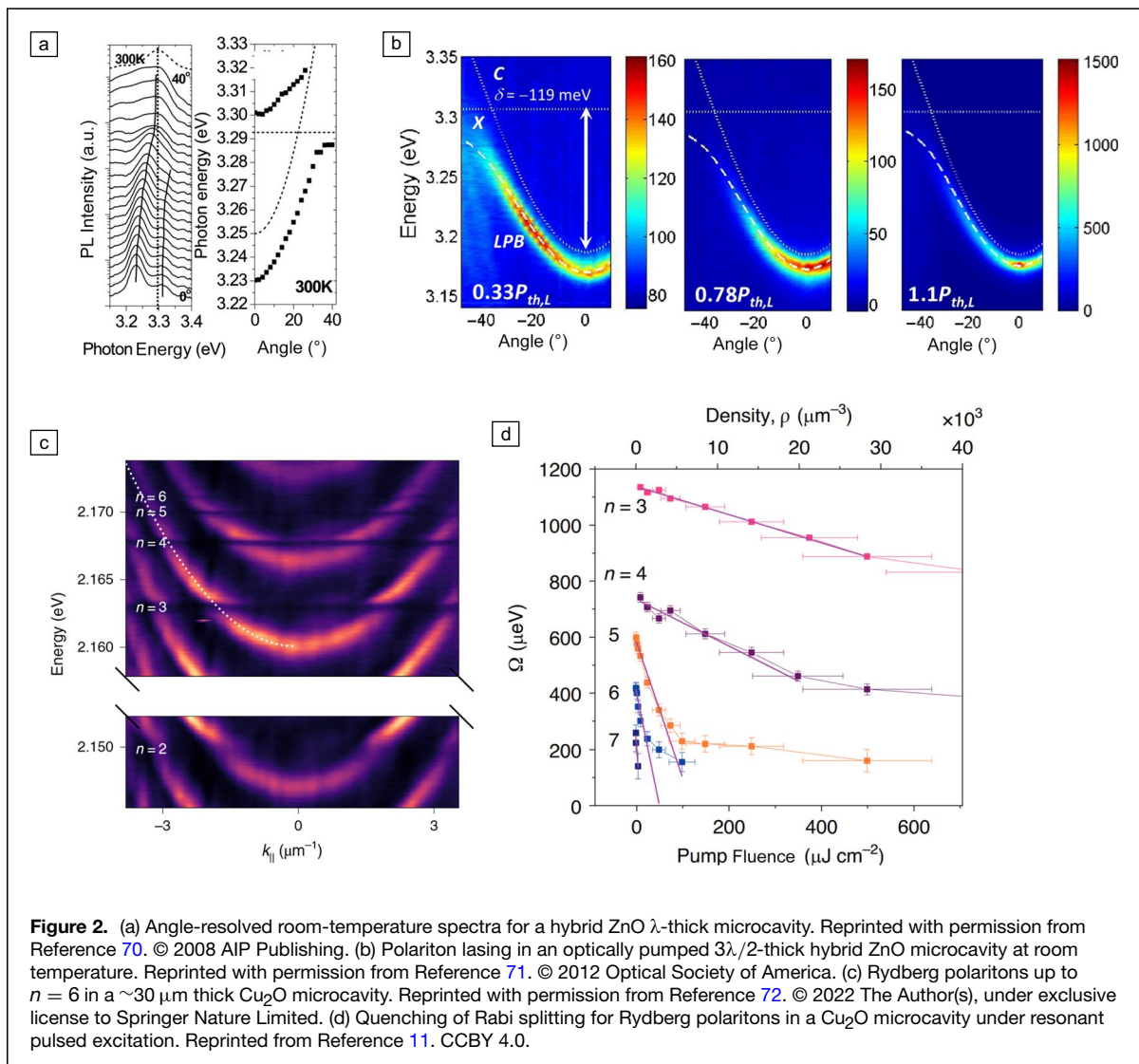
A resurgence in ZnO research emerged in the 2000s,[74] driven by advancements in nanostructure growth techniques, including epitaxial layers, quantum wells, nanorods, and quantum dots. ZnO, with its superior oscillator strength and higher exciton binding energy compared to GaN's 26 meV in bulk form, emerged as a preferred choice for room-temperature

polariton applications from an early stage.[75] The pioneering demonstration of strong exciton–photon coupling in ZnO was achieved in a layer grown by plasma-assisted molecular beam epitaxy within a hybrid microcavity composed of AlGaN/GaN and SiO_2/Si_3N_4 distributed Bragg reflectors (DBRs), revealing a vacuum Rabi splitting (VRS) of $\sim$50 meV at room temperature. An example is given in **Figure 2**a. This milestone was swiftly followed by comparable achievements in $3\lambda/2$ cavities, demonstrating similar VRS energies.[76] Further exploration into strong coupling with multiple quantum wells was undertaken, though sustaining this at room temperature proved challenging.[77]

Historically, vertical cavity surface emitting lasing was observed before the identification of polariton lasing.[78] Inventively, these structures incorporated eight quantum wells, opting for ZnO and its Mg alloys over bulk materials, and were encapsulated within ZnMgO alloy DBRs. These monolithic

ZnO-based microcavities demonstrated lasing under pulsed optical excitation, see Figure 2b, setting the stage for subsequent demonstrations of polariton lasing/condensation in bulk ZnO cavities at room temperature.[71,79] Remarkably, 1D ZnO cavities showcased polaritons with VRS reaching up to $\sim$ 300 meV,[80,81] a feature of ZnO that stands in contrast to other inorganic semiconductors such as GaAs, due to the VRS's comparability to LO-phonon energy. This facilitates polariton relaxation assisted by LO phonons.[82]

Further advancements were seen in the domain of ZnO microwires, where long-range spatial coherence and polariton lasing were first observed[83] before achieving polariton lasing at temperatures as high as 450K[84] and ZnO-based waveguide polariton lasing.[85] ZnO microrods, in particular, have shown exceptional promise in polariton physics, outpacing their 2D counterparts. Significant progress has been made in pattern formation and 1D lattices using ZnO microrods on gratings,[86] which

Figure 2. (a) Angle-resolved room-temperature spectra for a hybrid ZnO λ-thick microcavity. Reprinted with permission from Reference 70. © 2008 AIP Publishing. (b) Polariton lasing in an optically pumped $3\lambda/2$-thick hybrid ZnO microcavity at room temperature. Reprinted with permission from Reference 71. © 2012 Optical Society of America. (c) Rydberg polaritons up to $n = 6$ in a $\sim$30 μm thick Cu_2O microcavity. Reprinted with permission from Reference 72. © 2022 The Author(s), under exclusive license to Springer Nature Limited. (d) Quenching of Rabi splitting for Rydberg polaritons in a Cu_2O microcavity under resonant pulsed excitation. Reprinted from Reference 11. CCBY 4.0.

recently enabled polariton switching at room temperature with unprecedented speeds.[87] However, akin to GaN, planar ZnO microcavities face challenges related to inhomogeneity and large disorder, which negatively impact the polariton lifetimes. In addition, the nonlinearity observed in ZnO, while similar to GaN, is weaker than that of GaAs, posing obstacles to the advancement of ZnO microcavities in keeping pace with the rapid development of GaAs-based microcavities in lattice physics.

Copper(I) oxide (Cu_2O) along with germanium dioxide (GeO_2), tin dioxide (SnO_2), titanium dioxide (TiO_2), and thallium halide oxides form a category of oxides characterized by a direct bandgap. However, the transition from the valence band to the conduction band is dipole forbidden due to parity conservation (parity-forbidden transitions), implying that S excitons are dipole forbidden. Notably, for principal quantum number $n \geq 2$, $L = 1$ states emerge with odd parity, known as p-states, which gain a minimal oscillator strength. This subtle oscillator strength, coupled with Cu_2O's substantial Rydberg constant, allows the fitting of numerous excitonic states before reaching the bandgap edge (the continuum state). The linewidth of the p-states decreases as $1/n^3$, a trend mirrored by the oscillator strength. Consequently, the resonance amplitudes theoretically remain constant. This has been observed to hold to a degree for states up to $n \sim 15$, beyond which the oscillator strength diminishes sharply due to defect interactions.

In addition, the p-states coexist with a broad phonon absorption background of nearly equivalent magnitude to the exciton absorption amplitudes, which induces losses that constrain the cavity finesse. The initial demonstration of strong coupling for Rydberg excitons, up to $n = 6$, was achieved through a top-down methodology.[72] It involves the polishing and thinning of a bulk crystal down to 30 microns, which was then adhered to a DBR, with another DBR layer deposited on the crystal's opposite side. The resulting polariton dispersion curves are presented in Figure 2c. This technique drew parallels to methods used by the zinc oxide (ZnO) community in the early 2000 s. The light–matter coupling constant adhered to the $1/n^3$ oscillator strength relationship, but it declined significantly after $n = 5$. Following this, nonlinear effects were showcased in a similar setup (using silver mirrors instead of dielectric DBRs) where the nonlinearity was indirectly measured as a quenching of the Rabi splitting,[11] as visible in Figure 2d. The nonlinear coefficient for $n = 7$ matched that of the GaAs polariton system, marking this as the only system to exhibit comparable nonlinearity to GaAs at such a low Rydberg state. This opens the door for further enhancements and achieving significant single-polariton nonlinearity, contingent upon addressing the phonon background issue.

Promising avenues to bypass this challenge include electromagnetic transparency,[88] although this is demanding as it necessitates two-photon excitation with the second photon at THz frequencies. Achieving single-polariton nonlinearity necessitates the cavity volume to match the Rydberg blockade volume, which underscores the importance of substantial advancements in material development. Considerable progress has been made in the domain of synthetic bulk crystals,[89] microcrystals,[90] and thin films.[91] However, the highest quality remains with natural crystals. For these materials to be effectively integrated into photonic devices, synthetic thin films must evolve to match the maturity level of other semiconductor materials such as GaAs. Recent innovations in the patterning of bulk crystals and the crafting of Cu_2O pillars[92] offer promising avenues for the construction of Cu_2O lattices. Such advancements not only pave the way for exploring strong correlations within these structures, but also mark a significant step toward harnessing the full potential of Rydberg polaritons for quantum applications.

Exciton–polaritons in TMD monolayers

Atomically thin 2D van der Waals (vdW) materials have become a ubiquitous platform for studying variety of optoelectronic phenomena.[93] The most widely studied vdW material in the context of exciton–polaritons is transition-metal dichalcogenides (TMDCs) having MX_2 stoichiometry, where M is a transition metal from group VI (M = Mo, W) and X is a chalcogen (X = S, Se, Te).[94] These semiconductors exhibit markedly distinct electronic and optical properties in the monolayer (2D) limit compared to their bulk. For example, they transition from indirect to direct bandgap in the monolayer limit thereby increasing their photoluminescence (PL) quantum yield by more than 1000 times, demonstrate second harmonic generation (SHG) in the monolayer limit owing to the broken inversion symmetry and robust valley degree of freedom allowing the use of circularly polarized light to address valley (in momentum space) specific carriers. The latter also gives access to spin-valley dynamics, which can be mapped onto exciton–polaritons. Additionally, owing to the reduced dimensionality, the excitons and exciton complexes (bi-excitons, trions, fermi-polarons) exhibit large binding energy allowing access to excitonic physics and polaritons even at room temperature. Finally, the large oscillator strength exhibited by the excitons results in 10–15% absorption at excitonic resonances, makes them ideally suited to study strong light–matter interaction. All of these features of excitons in TMDCs can be imparted to their cavity polariton version, making them distinct from materials systems that have been studied extensively in the past such as GaAs and organic semiconductors. In some sense the properties of the TMDC excitons although describable within the Wannier-Mott (WM) picture can be thought of as having characteristics somewhere between the delocalized WM excitons of GaAs and highly localized Frenkel excitons found in organic molecules. Indeed, such hybrid features were considered in the past as a novel route to highly nonlinear polaritons.[95] Furthermore, the possibility to pick and place the 2D materials on different substrates presents a unique opportunity for integration of excitonic materials with photonic structures. Initial demonstrations of polaritons in 2D TMDCs were carried out using distributed Bragg reflector (DBR)-based Fabry–Perot (FP) cavities where the top mirror was either monolithically integrated[96] or in an open cavity

geometry where the top DBR was externally controlled.[97] Following these initial experiments, various geometries, including hybrid cavities consisting of DBR-metal structures as well as exfoliated and transferred top DBRs were used to demonstrate strong coupling.[98] The biggest challenge in realizing a DBR-DBR microcavity structure in the context of 2D semiconductors is their sensitivity to fabrication processes causing detrimental effects on the overall optical properties of the excitons. An attractive approach in this context are structures such as photonic crystals, plasmonic structures and metasurfaces that support coupling of their electromagnetic modes to the 2D excitons just by proximity[99] and does not require post-processing after the transfer of 2D materials. In almost all strong coupling experiments reported to date the 2D materials were exfoliated from bulk crystals or removed from a substrate following CVD growth and transferred onto the desired substrate using dry transfer techniques.[100] Owing to the large

refractive index of the TMDCs arising from the strong excitonic resonance,[101] these materials in their bulk form can host FP modes even without any mirrors and what is more intriguing is that these FP modes can self-hybridize with the excitons forming exciton–polaritons[102,103] (see **Figure 3**k). However, in this case, owing to the indirect bandgap of most bulk TMDCs, the polariton states can only be observed in absorption (reflection or transmission) and not in PL with ReS_2 and $ReSe_2$ being some of the exceptions. Nevertheless, their nonlinear optical response and potential to realize active metasurfaces have become active areas of research.[104–107]

The manifestation of strong coupling in 2D semiconductors nowadays goes beyond the mere observation of anticrossing: the advantage of 2D TMDs as polaritonic material can be seen in the wide array of novel phenomena and functions demonstrated. Next, we discuss some of the key effects:
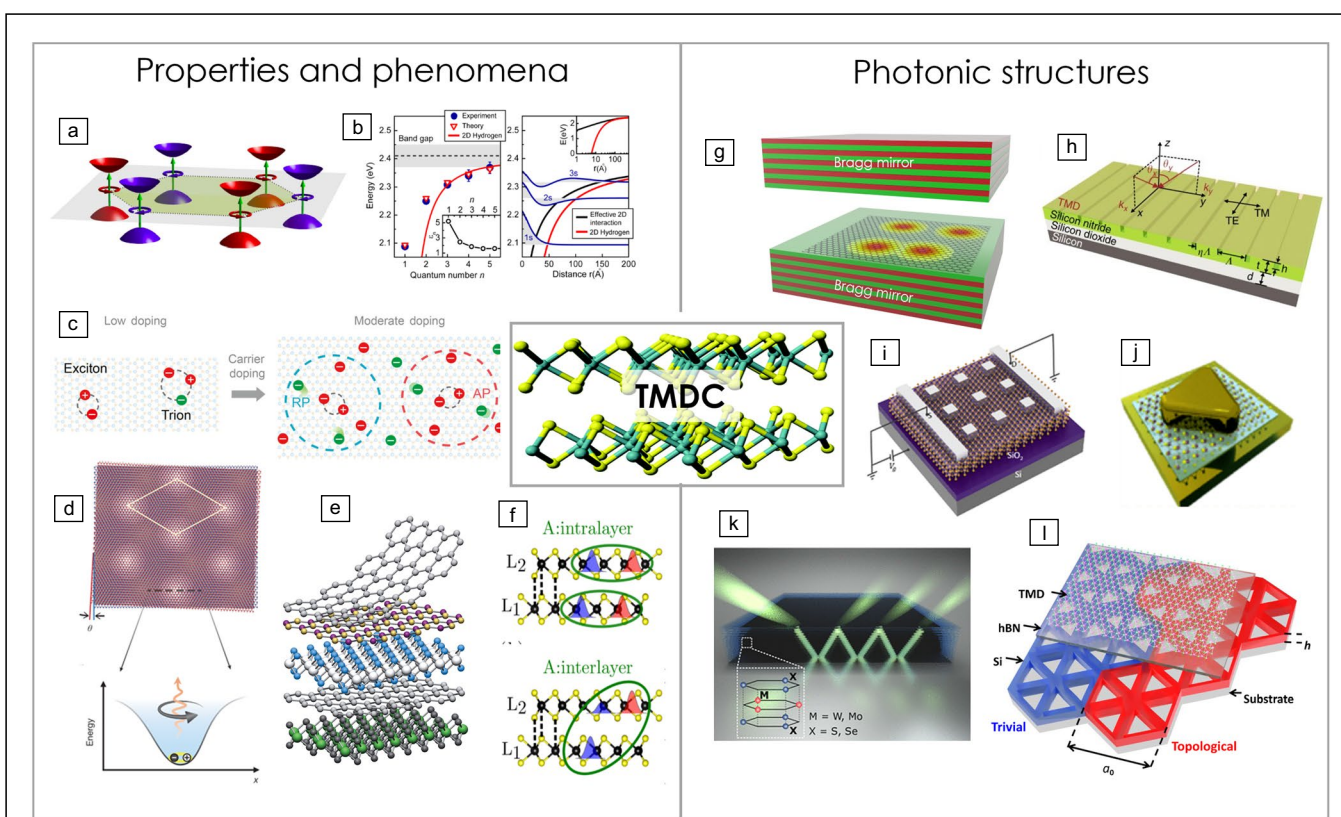

Figure 3. Properties and unique phenomena of TMDCs for exciton–polariton studies (Left panel) as well as the photonic structures that enable the realization of polaritons (Right panel). (a) Valley polarization property. Reprinted with permission from Reference 108. © 2014 Springer Nature. (b) Rydberg excitons observable due to the large binding energy. Reprinted with permission from Reference 109. ©2014 American Physical Society. (c) Charged excitons–trions and Fermi-polarons. Reprinted from Reference 110. CCBY 4.0. (d) Moiré excitons. Reprinted with permission from Reference 111. © 2019 Springer Nature. (e) Van der Waals heterostructures. Reprinted with permission from Reference 112. © 2013 Springer Nature. (f) Dipolar interlayer excitions. Reprinted with permission from Reference 113. © 2021 Springer Nature. (g) Bragg reflector-based 1D cavity. Reprinted with permission from Reference 96. © 2014, Springer Nature Limited. (h) Photonic crystal. Reprinted from Reference 99. CCBY 4.0. (i) Plasmonic array. Reprinted with permission from Reference 114. © 2020 American Chemical Society. (j) Nanoparticle on mirror. Reprinted with permission from Reference 115. © 2020 American Physical Society. (k) Self-hybridized polaritons. Reprinted with permission from Reference 102. © 2019 American Chemical Society. (l) Topological photonic crystals. Reprinted from Reference 116. CCBY 4.0.

Valley polarization and valley coherence: The valley degree of freedom relates to the quantum mechanically distinct valleys (minimas) in the momentum space that the electron occupies. In monolayer TMDCs, the direct bandgap occurs at the K and K' points and have distinct optical selection rules arising from the valley contrasting spin splitting of the valence and conduction bands,[108] as visible in Figure 3a. This allows one to excite the distinct valleys using circularly polarized light of specific handedness and results in the PL having predominantly the same handedness as the excitation laser and is termed "valley polarization." A related process termed "valley coherence" occurs under linear-polarized excitation which excites carriers in both valleys, and the resulting luminescence follows the linear polarization of the excitation laser. Magnetic fields have been used to rotate the linear polarization— thereby providing the possibility to control the valley pseudospin on demand. A similar effect was also observed under optical Stark effect. Such rotation of the valley pseudospin can be mapped onto a Bloch sphere and, hence, is analogous to spin state manipulation. There have been several reports of valley polarization being preserved and in fact in some cases even enhanced.[21,117–119] In all these reports, the cavity-modified exciton relaxation affects the valley depolarization of the excitons. Furthermore, this effect was found to depend on the exciton and photon fraction of the polariton. In addition to the Maialle–Silva–Sham (MSS) mechanism, the splitting between the transverse electric (TE) and transverse magnetic (TM) modes of the FP cavity also contribute to the overall valley depolarization of the polaritons. Valley coherence was also observed in polaritons formed in 2D TMDCs.[120–124] It was found that the polariton formation minimized valley dephasing. The control of polariton valley pseudospin using magnetic field was also demonstrated. In addition to exciton LT splitting, in the context of exciton–polaritons, one needs to also consider the TE-TM splitting of the cavity photon mode which results in a pseudomagnetic field that modifies the polarization properties.[125] Indeed, this effect has been recently used to manipulate valley coherence, where the dependence of TE-TM splitting on in-plane momentum ($k_{\parallel}$) was used to demonstrate precession of the valley pseudospin.[126,127] Another intriguing effect arising from the robust valley degree of freedom is the valley Hall effect, where the helicity of the pump photon can drive carriers from specific valleys (k or k') in opposite directions. In a recent demonstration, the valley-dependent directional propagation of polaritons in 2D TMDCs was demonstrated.[121]

Trion polaritons and Fermi-polaron polaritons: In the presence of doping, excitons are dressed by the Fermi sea, which allows the formation of trions (charged excitons, see Figure 3c) and Fermi-polarons at small and large doping, respectively. Owing to the large binding energy and oscillator strength of excitons in TMDCs, these exciton complexes have sufficient binding energy ($\sim$ 30 meV) and oscillator strength allowing them to strongly couple to cavity fields.[97,128] The use of doping of the TMDC layers via gating was also shown to tune strong coupling.[129] Polaritons formed from these charged excitonic complexes are especially interesting from the standpoint of nonlinearity owing to the Coulomb interaction.[130–132]

Nonlinear polariton–polariton interaction: Nonlinear interaction between polaritons is a key for realizing quantum nonlinearity as well as for Bose–Einstein like condensates. The primary mechanisms that dictate this interaction in monolayer TMDCs has been identified as phase space filling, and a smaller contribution from exchange interactions.[98,133,134] Following theoretical predictions,[135] polariton formation with the Rydberg excitonic states (Figure 3b) was demonstrated and the scaling of the nonlinearity with Bohr radius was shown.[17] Another intriguing possibility is the realization of polaritons using moiré excitons (Figure 3d) and interlayer excitons realized in vdW heterostructures (Figure 3e). A challenge there is usually the weak oscillator strength of these excitonic species owing to the predominantly out of plane dipole moment preventing the realizing of strong coupling. One solution is to use moiré excitons that are hybridized with intralayer excitons. This strategy was shown to be successful in realizing moiré exciton–polaritons with large nonlinear interaction strength attributed to the localized excitons at the moiré sites.[136] More recently, interlayer excitons with significantly large oscillator strength ($\sim$30% of the 1 s exciton) were shown to exist in homobilayer MoS_2[137] (Figure 3f) and were used to demonstrate highly nonlinear dipolar polaritons with one of the highest reported nonlinear interaction strengths.[138] The issue, however, is the linewidth of these interlayer excitons, which has so far been detrimental in reaching the limit of few photon nonlinearity.

Polariton condensation: Recently, there have been few reports of polariton condensation and onset of coherence in TMDC-based exciton–polaritons.[139–141] Although the binding energy of these excitons allows for condensation to be realized at room temperature, the initial experiments had to be carried out at low temperature most likely due to the sample quality. More recently, there have been reports of room-temperature condensation as well.[142,143] A related work showed the emergence of spatial coherence in 2D TMDC-based cavity structures owing to the spatial inhomogeneity and the small flake size.[144] A significant challenge in using such 2D TMDC-based BECs for realizing condensate lattices or other polaritonic structures is the small size of the exfoliated flakes. Using high-quality CVD grown flakes or the use of gold exfoliation technique could address this issue.[145]

Photonic and plasmonic crystal-based polaritons: By exploiting the possibility to pick and place the 2D material on different structures, various groups have reported realizing exciton polaritons using photonic crystals and plasmonic lattices[99,146,147] (see Figure 3h–i). These structures allow larger tunability of the photonic dispersion as well as the Q-factor, which maps on to the polaritons as well. A good example of this is the coupling of excitons in TMDCs to topological photonic crystals. Here, the polariton emission was shown to couple in a nonreciprocal manner owing to the band structure of

the underlying photonic crystal,[116,148] see Figure 3l. The ability to realize vdW heterostructures also allowed the realization of an electrically driven polariton LED which consisted of thin hBN tunnel barriers, graphene contact, and WS_2 as the excitonic emitter. The entire structure consisted of eleven layers and was placed inside a DBR—silver cavity.[17]

Outlook

Looking ahead, some of the new directions include the possibility of reaching the polariton blockade limit by exploiting the enhancement in nonlinearity provided by the TMDCs via the various mechanisms such as dipolar interactions, coulomb interaction arising from charged excitons, or even large Bohr radius Rydberg excitons, as visible in Figure 3b. A recent direction that has emerged is the use of correlated vdW materials such as charge-transfer insulators[149] and vdW magnets.[150] In these systems, the intertwined electronic, magnetic, and optical responses present

a unique opportunity to explore the role of strong coupling and the distinctive properties of this new class of exciton–polaritons.

Exciton–polaritons in halide perovskite semiconductors

Halide perovskites represent an emerging class of semiconductors that can be processed from solutions at temperatures below 100°C and ambient pressure. This method is well suited for low-cost and large-surface applications. The so-called 3D perovskites (see **Figure 4**a), with a general chemical formula of ABX_3 (where A is a cation, B is a divalent metal such as Pb, and X is a halogen such as I, Br, or Cl) are direct band-gap semiconductors and stand out due to their remarkable chemical flexibility, enabled by soft chemistry techniques. Each component—A, B, and X—can be customized: A can range from organic compounds such as methylammonium $[MA = (CH_3NH_3^+)]$ to inorganic elements such as Cs, or even
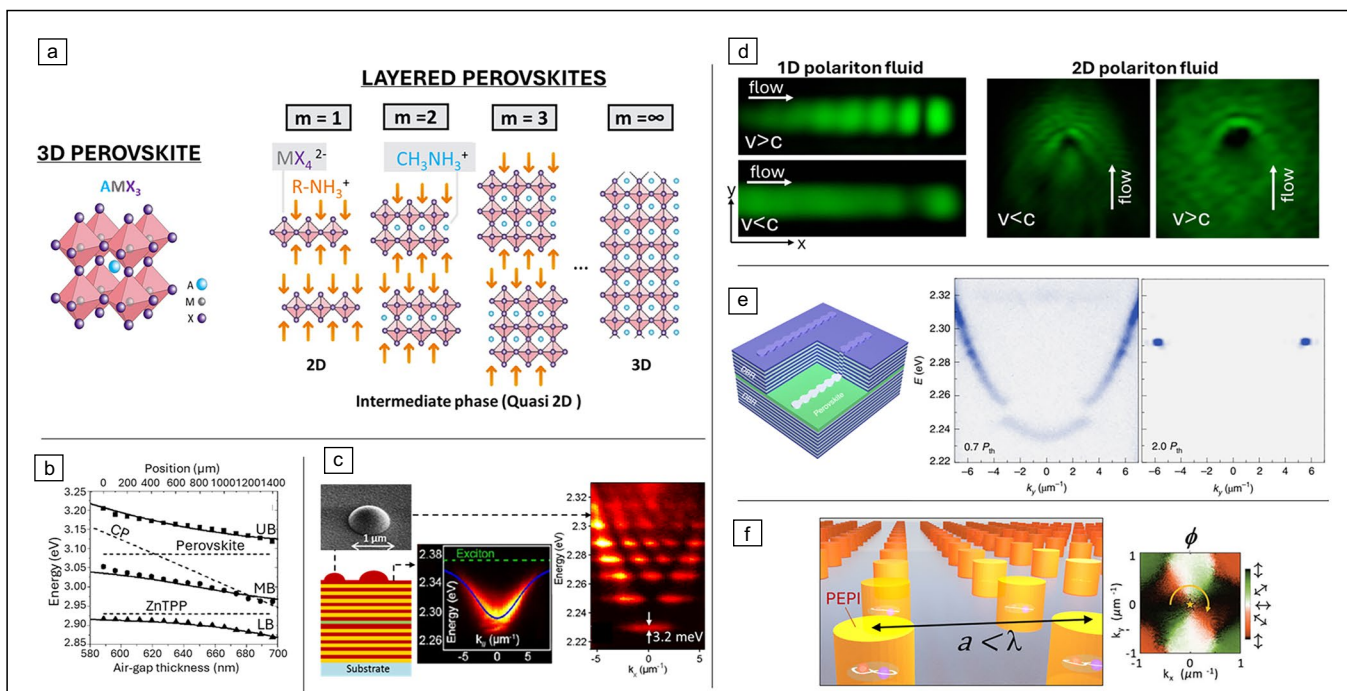

Figure 4. (a) Crystalline structure of (Left) 3D perovskites, and (Right) layered Ruddlesden–Popper perovskites. (b) Energy of the three polariton branches of the hybridization between cavity photons (CPs), perovskite excitons, and ZnTPP when scanning the cavity air gap. Reprinted with permission from Reference 151. © 2006 American Physical Society. (c) Left panel: 2D microcavity and 0D photonic molecule on the same sample with PEPI as an active layer. The SEM image shows a sphere-like 0D photonic molecule on the top-mirror. Middle and Right panels: Polariton dispersion measured in the 2D cavity region and the 0D photonic molecules, respectively. Reprinted with permission from Reference 152. © 2014 AIP Publishing LLC. (d) Images of nonlinear polariton transport for 1D (left) and 2D (right) fluids, illustrating supersonic and subsonic propagation. Reprinted from Reference 153. CCBY 4.0. In the supersonic regime, the 1D fluid exhibits patterns originating from the interference between the flow and its reflection at the sample edge, while the 2D fluid shows Cerenkov waves upon encountering a defect. In the subsonic regime, the absence of scattering in both 1D and 2D fluids indicates their superfluid nature. (e) Left: Sketch of a mono-atomic polaritonic chain made of perovskite-based coupled micropillars. The lattice confinement was achieved by introducing a patterned PMMA layer on top of the $CsPbBr_3$ flake. Middle and right panels: Polariton dispersion measured at pump power below and above the threshold, respectively. Reprinted from Reference 154. CCBY-NC 4.0. (f) Left: Sketch of a perovskite metasurface composed of subwavelength PEPI pillars arranged in a square lattice with subwavelength periodicity. Reprinted with permission from Reference 155. © 2020 American Chemical Society. Right: Experimental results showing the measurement of the polarization orientation angle ϕ, demonstrating the polarization singularity at a polariton bound state in the continuum. Reprinted with permission from Reference 156. © 2022 Wiley.

combinations thereof. B can be a single divalent metal or a blend between two cations. X can be any combination of halogen ions. Adjusting the halogen content in lead-based perovskites allows for the tuning of the perovskite's bandgap across the visible spectrum. Most importantly, by tuning the component A and the stoichiometry of the mixture, perovskites can be engineered into lower-dimensional forms. For instance, the layered perovskites, among the most studied, of general formula $(R-NH_3)_2(CH_3NH_3)_{m-1}M_mX_{3m+1}$ (see Figure 4a), are synthesized by incorporating bulky organic components such as phenylethylammonium $[PE = (C_6H_5C_2H_4NH_3^+)]$. Varying the integer m allows for control over the material's excitonic characteristics. At $m = 1$, the structure is 2D, confining both electrons and holes within an atomically thin inorganic layer composed of $[PbX_6]^{4-}$ octahedra (type-I quantum well). This configuration results in strongly bound excitons with binding energies of several hundred meV due to quantum and dielectric confinements.[157] Conversely, at $m = \infty$, the material transitions to a 3D structure ($MAPbX_3$), characterized by weaker excitons. Thus, from $m = 1$ to $m = \infty$, the excitonic properties of hybrid perovskites can be continuously tailored.[158]

Exhibiting superior excitonic effects compared to other members of its family, the 2D hybrid perovskite ($m = 1$) is naturally the most suitable layered perovskite for studying the exciton–photon strong coupling regime. In 1998, the strong coupling regime using perovskite material was demonstrated for the first time, employing a spin-coated layer of PE_2PbI_4, known as PEPI in a distributed feedback cavity at room temperature.[159] Subsequently, single-mode planar microcavities with a 50-nm spin-coated layer of PEPI showcased strong coupling at room temperature with substantial Rabi splittings of 150 meV.[160] This is facilitated by 1) the remarkably stable exciton with a binding energy of more than 200 meV; 2) a high oscillator strength (optical coupling strength) of 3.6×10^{13} cm^{-2} per quantum well. Notably, the interaction between the photonic mode and the perovskite, alongside another material with a high excitonic oscillator strength, results in the formation of three-component hybridized states[151] (see Figure 4b).

Unlike other room-temperature polariton materials, perovskites produce delocalized Wannier excitons with a Bohr radius significantly larger than the material's lattice period, promising high nonlinearity. Investigations into the excitonic nonlinearities of PEPI have revealed behaviors similar to those of GaAs-based semiconductors, despite PEPI's high exciton binding energy.[161] Remarkably, the exciton–exciton interaction energies, derived from the polariton nonlinearity in PEPI-based polaritons, are spin dependent and closely resemble those observed in GaAs-based quantum wells at cryogenic temperatures exceeding those of organic polaritons by more than an order of magnitude.[162] Furthermore, coupling of photons in engineered 0D microcavity with PEPI excitons, polaritonic mode of experimental Q-factor up to 750 was reported[152] (see Figure 4c). Despite these promising features, leveraging 2D hybrid perovskites to achieve polariton BEC at room temperature remains a significant challenge due to strong

surface trapping, long-lived triplet states, Auger recombination, and exciton–phonon interactions. To date, BEC has only been experimentally demonstrated at cryogenic temperatures for these materials.[163]

Using 3D all-inorganic perovskites, researchers finally solved the puzzle of creating a polariton BEC at room temperature from a halide perovskite material. This breakthrough was made possible by a tradeoff between the lower excitonic confinement, which leads to smaller exciton binding energy, and the superior gain properties of 3D all-inorganic perovskites compared to their 2D hybrid counterparts. The first observation of polariton BEC at room temperature in perovskite materials was demonstrated with a planar microcavity containing an exfoliated $CsPbCl_3$ flake.[164] Using the same platform, but with 1D exfoliated $CsPbBr_3$, long-range coherent propagation of a polariton condensate was subsequently reported.[165] In addition, hallmarks of nonlinear polaritons such as optical parametric scattering[166] and nonlinear transport of quantum fluid[153](see Figure 4d) were demonstrated with this platform. Remarkably, in the same fashion as cryogenic polaritons in GaAs systems, a tight-binding Hamiltonian can be engineered using coupled micropillars of a perovskite-based cavity. This is achieved by implementing a patterned PMMA layer on top of the perovskite flake before the deposition of the top Bragg mirror. For instance, polariton BEC in a polariton monoatomic chain[154] (see Figure 4e) and at the topological edge state of a Su–Schrieffer–Heeger (SSH) chain[167] were demonstrated. However, a recent report casts doubt on whether the observed polariton BECs with all-inorganic perovskites were actually below the Mott density threshold, suggesting that the lasing emissions may originate from polaritonic Bardeen–Cooper–Schrieffer states rather than polariton BEC.[168] Therefore, further studies investigating the photophysics of polariton lasing in all-inorganic perovskites are crucial.

Despite the success of 3D all-inorganic perovskites in achieving perovskite-based polariton BEC at room temperature, most of these studies employed perovskite flakes that were exfoliated. However, creating solution-based thin films of these perovskites is challenging due to the low solubility of CsBr and CsI precursors, which hinders the production of large surface polaritonic devices. To overcome this limitation, using spin-coated 3D hybrid perovskites instead of exfoliated 3D all-inorganic perovskites presents a promising alternative. Indeed, strong coupling has been demonstrated in a planar microcavity with a spin-coated $MAPbBr_3$ layer.[169] While the low Q-factor ∼100 of this structure does not lead to polariton lasing, the polaritonic modes have been utilized to redirect the random lasing emission for directional beam.[170]

Finally, the integration of superior excitonic features of perovskite materials with modern nanophotonic concepts, including bound states in the continuum and exceptional points in subwavelength metasurface lattices,[171] is a promising strategy for novel polaritonic functionalities. These metasurfaces are composed of perovskite elements not only of subwavelength

size but also arranged with a subwavelength periodicity (see Figure 4f). They can be fabricated by infiltrating a perovskite solution into a prepatterned substrate[155] or through direct nano-imprinting.[172] Milestones of strong coupling physics with perovskite metasurface include (1) on-demand dispersion engineering of polaritonic modes;[155] (2) formation of polariton bound states in the continuum, which significantly enhances the Q-factor and exhibits polarization singularity[156] (see Figure 4f); and (3) polariton lasing at exceptional points.[173] Most recently, large-scale perovskite metasurfaces were constructed using cost-effective methods such as interference lithography, spin coating, and thermal nanoimprint, showcasing homogeneous polaritonic modes across cm^2 of sample area.[172]

Exciton–polaritons in organic semiconductors

The first demonstration of cavity polaritons with an organic material, has been performed by Lydzey et al. in Reference 174. The cavities studied were produced by spin coating an organic layer (porphyrin molecules in a polystyrene matrix) onto a Bragg mirror, the cavity being closed by a metal mirror. Reflectometry experiments at room temperature have shown the typical anticrossing between optical resonance and organic exciton with a Rabi splitting of 160meV. One year later strong coupling was evidenced with Cyanine J-aggregated dyes excitons.[175] These first demonstrations highlighted two of the key properties of organic polaritons: the large light–matter coupling strength (oscillator strength) of organic semiconductors, which means they can operate at room temperature and the relative simplicity of fabricating the structures (compared with epitaxial GaAs structures). Since then, a wide variety of organic materials have been exploited for polaritons, including molecules in matrix,[176] J-aggregated dyes,[175] polymers,[9] fluorescent proteins[177] and organic crystals.[178] The Rabi oscillation between exciton and photons that is intrinsically linked to strong coupling, was observed with pump probe experiments with J-aggregates excitons coupled to metal nanostructure resonances.[179] Ultrafast oscillations a period of a few tens of femtoseconds, were associated with the large Rabi energy of organic polaritons. It should be noted that recently, organic polaritons in the infrared range have been demonstrated by coupling a vibrational transition (c = o stretching), instead of an excitonic transition, to a cavity mode.[180]
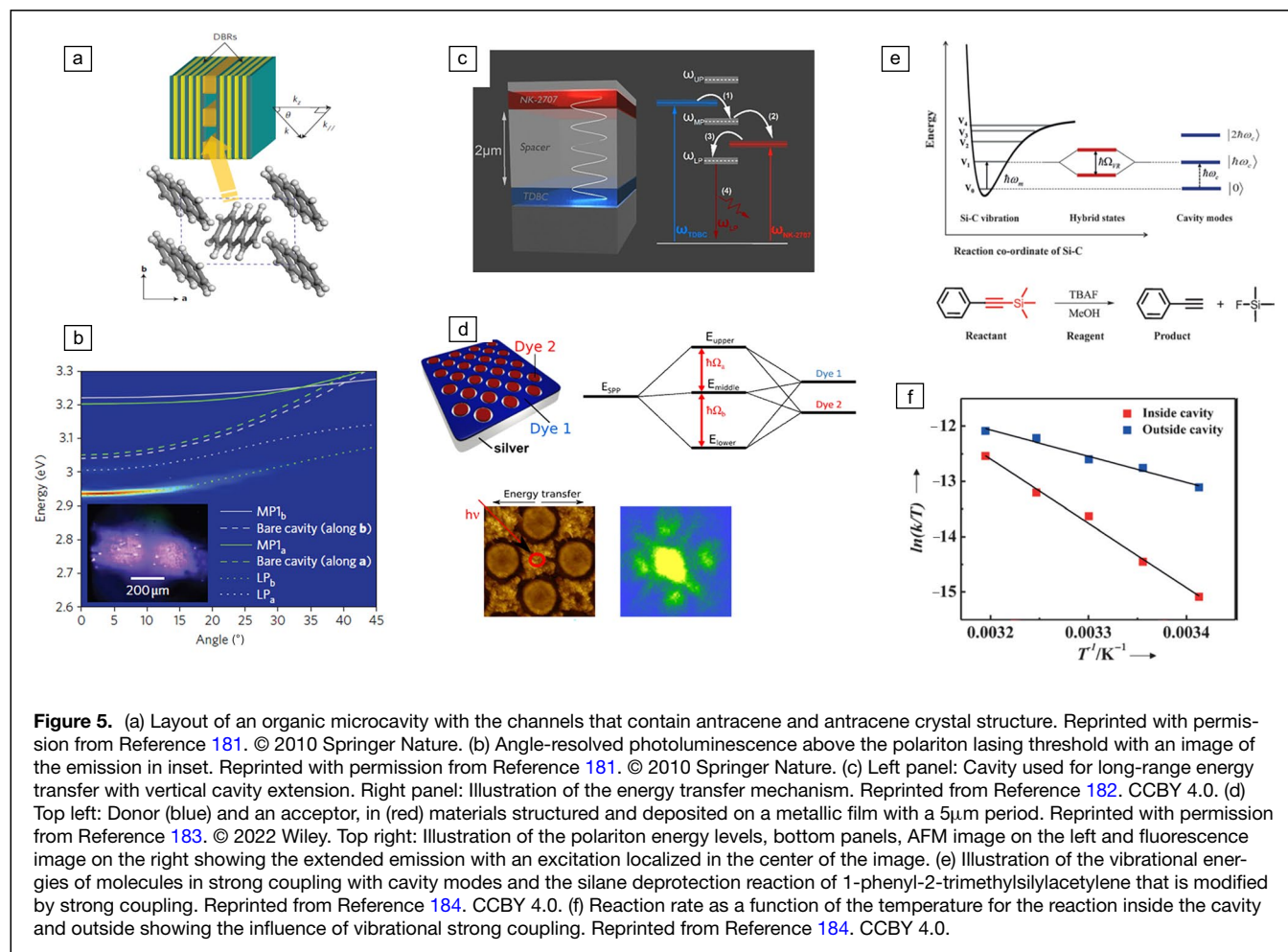
The excitons (electron and positively charged vacancy linked by a Coulomb interaction) in these organic materials with different degrees of order, from single molecules to molecular crystals, are highly localized with respect to the photon wavelength.[185] They can, therefore, be considered to be dispersionless, and thus, differ from extended Wannier excitons in inorganic semiconductors. The image of a photon and an exciton with the same in-plane wave vector hybridizing to create a polariton[22] is no longer relevant. Agranovich et al. have theoretically studied the structure of polaritons[185] in disordered organic semiconductors (J-aggregated dye).

Considering the material excitations as localized point dipole moments spread in the cavity, the system supports coexisting coherent and incoherent excitations. Coherent states are superposition of a photon and excitons of a large number of molecules, with a well-defined wavevector. The extended coherence of excitons that spread on several microns has been experimentally demonstrated.[186] Incoherent states are formed by a superposition of excitons that are dispersionless and spectrally close to the bare exciton energy.[187] These incoherent states, also named exciton reservoir, play a key role in relaxation in organic systems in strong coupling.[188]

As the oscillation strength of organic materials is large, high-quality resonators are no longer needed to generate polaritons. Hybrid states between organic excitons and propagating surface plasmon modes have been demonstrated in 2004.[189] A J-aggregated dye layer deposited on a silver film that supports surface plasmons constituted only the system studied. Different localized plasmon resonances have also been hybridized with excitons (a review can be found in Reference 190). Polaritons can even be generated in free standing membranes without mirror (Q-factor = 33).[191] Several applications of polaritons require low-loss optical modes. In addition to microcavities with Bragg mirrors, low losses modes have been proposed, such as plasmonic gratings[192] as well as dielectric resonator arrays[193] or Bloch surface waves.[194]

The inclusion of two or more different materials in a strongly coupled cavity under appropriate conditions leads to the formation of hybrid states that mix the excitons of each material.[195] One particular application of this hybridization is to improve the energy transfer between a donor material and an acceptor material. Energy is transferred through an intermediate state comprising the contributions of both donor and acceptor (medium-energy polariton).[196] As long as the donor and acceptor are hybridized together by the optical mode, energy transfer remains efficient. This nonradiative energy transfer in strong coupling has been demonstrated for separations of up to 100 nm, with time-resolved experiments.[197] This distance should be compared with a few tens of nanometers for Forster energy transfer. The transfer distance can be increased to several microns by extending the cavities vertically[182] (see **Figure 5**c) or by using the lateral extension of the optical mode. Indeed, structuring an organic layer on a metal film (plasmon mode) leads to a metasurface effect, if the spatial period is smaller than the polariton extension.[198] In order to couple two materials, two patterned interlocked dyes arrays, one donor and one acceptor, need to be deposited on a silver film, as illustrated in Figure 5d. For a period of 5 μm, the donor and acceptor are hybridized by plasmon, leading to long-range energy transfer.[183]

The room-temperature polariton laser is an important application of the organic polaritons. Polaritonic condensed emission was first demonstrated in a highly ordered organic material, anthracene single crystal, sandwiched between two Bragg mirrors.[181] The emission as a function of the pump fluence passes from a sublinear level (bimolecular extinction) to

Figure 5. (a) Layout of an organic microcavity with the channels that contain antracene and antracene crystal structure. Reprinted with permission from Reference 181. © 2010 Springer Nature. (b) Angle-resolved photoluminescence above the polariton lasing threshold with an image of the emission in inset. Reprinted with permission from Reference 181. © 2010 Springer Nature. (c) Left panel: Cavity used for long-range energy transfer with vertical cavity extension. Right panel: Illustration of the energy transfer mechanism. Reprinted from Reference 182. CCBY 4.0. (d) Top left: Donor (blue) and an acceptor, in (red) materials structured and deposited on a metallic film with a 5μm period. Reprinted with permission from Reference 183. © 2022 Wiley. Top right: Illustration of the polariton energy levels, bottom panels, AFM image on the left and fluorescence image on the right showing the extended emission with an excitation localized in the center of the image. (e) Illustration of the vibrational energies of molecules in strong coupling with cavity modes and the silane deprotection reaction of 1-phenyl-2-trimethylsilylacetylene that is modified by strong coupling. Reprinted from Reference 184. CCBY 4.0. (f) Reaction rate as a function of the temperature for the reaction inside the cavity and outside showing the influence of vibrational strong coupling. Reprinted from Reference 184. CCBY 4.0.

a super-linear level after the lasing threshold. An accumulation at the bottom of the dispersion, associated with extended spatial coherence,[199] also occurs above threshold (see Figure 5b). BEC has been demonstrated in various organic materials that are less ordered than anthracene single crystals (review articles on organic polariton laser can be found in References 200 and 201), but also in plasmonic structures based on plasmonic lattice resonances.[202] The reduction of the polariton laser threshold can be achieved by improving the relaxation processes from the exciton reservoir to the low energy polariton.[203]

In the last 10 years, a new direction has emerged with organic polaritons, building on the pioneering work of Ebbesen et al.,[204] which aims to exploit the strong coupling between light and matter to modify the properties of these materials beyond their optical properties.[205] Strong interaction with a resonant mode modifies the molecular states (associated with a resonant transition with the optical mode), with a change in energy landscape and the formation of coherent extended states. These modifications are perceptible either by direct optical measurement or without light, through changes in "nonoptical" material properties. The electrical conductivity of an organic film can be improved by one order of magnitude when it is strongly coupled to a plasmonic resonator.[204] Chemical reactivity can also be modified with strong coupling between a cavity mode and excitonic transition[206] or vibronic transitions,[207] as illustrated in see Figure 5e–f. In addition to new applications for organic polaritons, these phenomena raise open theoretical questions that are the subject of numerous studies.[208]

Conclusion

In this article, we have explored some of the diverse landscape of semiconductor materials that can be utilized for exciton–polaritons, highlighting their respective advantages and challenges. By leveraging the diversity of semiconductors, one can tailor the properties of exciton–polaritons to suit specific applications and explore novel phenomena. Therefore, exciton–polaritons in semiconductor microcavities represent more than ever a captivating frontier at the intersection of quantum mechanics, condensed-matter physics, and photonics. Through continued research and technological advancements, exciton–polaritons are poised to play a significant role in shaping the future of photonics and quantum technologies.

Author contributions
All authors contributed equally.

Data availability
Not applicable

Conflict of interest
The authors declare having no conflict of interest.

References
1. I. Carusotto, C. Ciuti, *Rev. Mod. Phys.* **85**, 299 (2013)
2. M.J. Jacquet, T. Boulier, F. Claude, A. Maître, E. Cancellieri, C. Adrados, A. Amo, S. Pigeon, Q. Glorieux, A. Bramati, E. Giacobino, *Philos. Trans. R. Soc. A* **378**, 20190225 (2020)
3. S.B. Anantharaman, K. Jo, D. Jariwala, *ACS Nano* **15**, 12628 (2021)
4. F.I. Moxley III., E.O. Ilo-Okeke, S. Mudaliar, T. Byrnes, *Emergent Mater.* **4**, 971 (2021)
5. A. Amo, J. Lefrère, S. Pigeon, C. Adrados, C. Ciuti, I. Carusotto, R. Houdré, E. Giacobino, A. Bramati, *Nat. Phys.* **5**, 805 (2009)
6. J. Kasprzak, M. Richard, S. Kundermann, A. Baas, P. Jeambrun, J.M.J. Keeling, F.M. Marchetti, M.H. Szymańska, R. André, J.L. Staehli, V. Savona, P.B. Littlewood, B. Deveaud, L.S. Dang, *Nature* **443**, 409 (2006)
7. K.G. Lagoudakis, M. Wouters, M. Richard, A. Baas, I. Carusotto, R. André, L.S. Dang, B. Deveaud-Plédran, *Nat. Phys.* **4**, 706 (2008)
8. A. Amo, S. Pigeon, D. Sanvitto, V.G. Sala, R. Hivet, I. Carusotto, F. Pisanello, G. Leménager, R. Houdré, E. Giacobino, C. Ciuti, A. Bramati, *Science* **332**, 1167 (2011)
9. J.D. Plumhof, T. Stöferle, L. Mai, U. Scherf, R.F. Mahrt, *Nat. Mater.* **13**, 247 (2014)
10. Z. Li, F. Claude, T. Boulier, E. Giacobino, Q. Glorieux, A. Bramati, C. Ciuti, *Phys. Rev. Lett.* **128**, 093601 (2022)
11. M. Makhonin, A. Delphan, K. W. Song, P. Walker, T. Isoniemi, P. Claronino, K. Orfanakis, S. K. Rajendran, H. Ohadi, J. Heckötter, M. Assmann, M. Bayer, A. Tartakovskii, M. Skolnick, O. Kyriienko, and D. Krizhanovskii, *Light* **13**, 47 (2024)
12. T. Boulier, M. Jacquet, A. Maître, G. Lerario, F. Claude, S. Pigeon, Q. Glorieux, A. Amo, J. Bloch, A. Bramati, E. Giacobino, *Adv. Quantum Technol.* **3**, 2000052 (2020)
13. G. Muñoz-Matutano, A. Wood, M. Johnsson, X. Vidal, B.Q. Baragiola, A. Reinhard, A. Lemaître, J. Bloch, A. Amo, G. Nogues, B. Besga, C. Gomez, A. Lemaître, J. Bloch, A. Amo, T. Volz, *Nat. Mater.* **18**, 213 (2019)
14. A. Delteil, T. Fink, A. Schade, S. Höfling, C. Schneider, A. İmamoğlu, *Nat. Mater.* **18**, 219 (2019)
15. A. Amo, T. Liew, C. Adrados, R. Houdré, E. Giacobino, A. Kavokin, A. Bramati, *Nat. Photonics* **4**, 361 (2010)
16. A. Kavokin, T.C. Liew, C. Schneider, P.G. Lagoudakis, S. Klembt, S. Hoefling, *Nat. Rev. Phys.* **4**, 435 (2022)
17. J. Gu, B. Chakraborty, M. Khatoniar, V.M. Menon, *Nat. Nanotechnol.* **14**, 1024 (2019)
18. M.D. Fraser, S. Höfling, Y. Yamamoto, *Nat. Mater.* **15**, 1049 (2016)
19. M. Liu, M. Jiang, Q. Zhao, K. Tang, S. Sha, B. Li, C. Kan, D.N. Shi, *ACS Appl. Mater. Interfaces* **15**, 13258 (2023)
20. R. Su, A. Fieramosca, Q. Zhang, H.S. Nguyen, E. Deleporte, Z. Chen, D. Sanvitto, T.C. Liew, Q. Xiong, *Nat. Mater.* **20**, 1315 (2021)
21. Y.-J. Chen, J.D. Cain, T.K. Stanev, V.P. Dravid, N.P. Stern, *Nat. Photonics* **11**, 431 (2017)
22. C. Weisbuch, M. Nishioka, A. Ishikawa, Y. Arakawa, *Phys. Rev. Lett.* **69**, 3314 (1992)
23. D. Sanvitto, S. Kéna-Cohen, *Nat. Mater.* **15**, 1061 (2016)
24. A. Kavokin, G. Malpuech, M. Glazov, *Phys. Rev. Lett.* **95**, 136601 (2005)
25. P.G. Savvidis, J.J. Baumberg, R.M. Stevenson, M.S. Skolnick, D.M. Whittaker, J.S. Roberts, *Phys. Rev. Lett.* **84**, 1547 (2000)
26. A. Baas, J.P. Karr, H. Eleuch, E. Giacobino, *Phys. Rev. A* **69**, 023809 (2004)
27. T. Boulier, M. Bamba, A. Amo, C. Adrados, A. Lemaitre, E. Galopin, I. Sagnes, J. Bloch, C. Ciuti, E. Giacobino, A. Bramati, *Nat. Commun.* **5**, 3260 (2014)
28. F. Tassone, C. Piermarocchi, V. Savona, A. Quattropani, P. Schwendimann, *Phys. Rev. B* **56**, 7554 (1997)
29. R. Balili, V. Hartwell, D. Snoke, L. Pfeiffer, and K. West, *Science* **316**, 1007 (2007), https://www.science.org/doi/pdf/10.1126/science.1140990
30. S. Christopoulos, G.B.H. von Högersthal, A.J.D. Grundy, P.G. Lagoudakis, A.V. Kavokin, J.J. Baumberg, G. Christmann, R. Butté, E. Feltin, J.-F. Carlin, N. Grandjean, *Phys. Rev. Lett.* **98**, 126405 (2007)
31. Q. Fontaine, D. Squizzato, F. Baboux, I. Amelio, A. Lemaître, M. Morassi, I. Sagnes, L.L. Gratiet, A. Harouri, M. Wouters, I. Carusotto, A. Amo, M. Richard, A. Minguzzi, L. Canet, S. Ravets, J. Bloch, *Nature* **608**, 687 (2022)
32. I. Carusotto, C. Ciuti, *Phys. Rev. Lett.* **93**, 166401 (2004)
33. F. Claude, M.J. Jacquet, I. Carusotto, Q. Glorieux, E. Giacobino, A. Bramati, *Phys. Rev. B* **107**, 174507 (2023)
34. C. Leyder, M. Romanelli, J.P. Karr, E. Giacobino, T.C.H. Liew, M.M. Glazov, A.V. Kavokin, G. Malpuech, A. Bramati, *Nat. Phys.* **3**, 628 (2007)
35. A. Gianfrate, O. Bleu, L. Dominici, V. Ardizzone, M.D. Giorgi, D. Ballarini, G. Lerario, K.W. West, L.N. Pfeiffer, D.D. Solnyshkov, D. Sanvitto, G. Malpuech, *Nature* **578**, 381 (2020)
36. T. Gao, E. Estrecho, K.Y. Bliokh, T.C. Liew, M.D. Fraser, S. Brodbeck, M. Kamp, C. Schneider, S. Höfling, Y. Yamamoto, F. Nori, Y.S. Kivshar, A.G. Truscott, R.G. Dall, E.A. Ostrovskaya, *Nature* **526**, 554 (2015)
37. C. Schneider, K. Winkler, M.D. Fraser, M. Kamp, Y. Yamamoto, E.A. Ostrovskaya, S. Höfling, *Rep. Prog. Phys.* **80**, 016503 (2016)
38. A. Amo, J. Bloch, *C. R. Phys.* **17**, 934 (2016)
39. F. Baboux, L. Ge, T. Jacqmin, M. Biondi, E. Galopin, A. Lemaître, L. Le Gratiet, I. Sagnes, S. Schmidt, H.E. Türeci, A. Amo, J. Bloch, *Phys. Rev. Lett.* **116**, 066402 (2016)
40. C.E. Whittaker, E. Cancellieri, P.M. Walker, D.R. Gulevich, H. Schomerus, D. Vaitiekus, B. Royall, D.M. Whittaker, E. Clarke, I.V. Iorsh, I.A. Shelykh, M.S. Skolnick, D.N. Krizhanovskii, *Phys. Rev. Lett.* **120**, 097401 (2018)
41. D. Tanese, E. Gurevich, F. Baboux, T. Jacqmin, A. Lemaître, E. Galopin, I. Sagnes, A. Amo, J. Bloch, E. Akkermans, *Phys. Rev. Lett.* **112**, 146404 (2014)
42. V. Goblot, B. Ŝtrkalj, N. Pernet, J.L. Lado, C. Dorow, A. Lemaître, L.L. Gratiet, A. Harouri, I. Sagnes, S. Ravets, A. Amo, J. Bloch, O. Zilberberg, *Nat. Phys.* **16**, 832 (2020)
43. T. Jacqmin, I. Carusotto, I. Sagnes, M. Abbarchi, D.D. Solnyshkov, G. Malpuech, E. Galopin, A. Lemaître, J. Bloch, A. Amo, *Phys. Rev. Lett.* **112**, 116402 (2014)
44. M. Milićević, G. Montambaux, T. Ozawa, O. Jamadi, B. Real, I. Sagnes, A. Lemaître, L. Le Gratiet, A. Harouri, J. Bloch, A. Amo, *Phys. Rev. X* **9**, 031010 (2019)
45. C.E. Whittaker, T. Dowling, A.V. Nalitov, A.V. Yulin, B. Royall, E. Clarke, M.S. Skolnick, I.A. Shelykh, D.N. Krizhanovskii, *Nat. Photonics* **15**, 193 (2021)
46. S. Klembt, T.H. Harder, O.A. Egorov, K. Winkler, R. Ge, M.A. Bandres, M. Emmerling, L. Worschech, T.C.H. Liew, M. Segev, C. Schneider, S. Höfling, *Nature* **562**, 552 (2018)
47. P. St-Jean, V. Goblot, E. Galopin, A. Lemaître, T. Ozawa, L.L. Gratiet, I. Sagnes, J. Bloch, A. Amo, *Nat. Photonics* **11**, 651 (2017)
48. N.C. Zambon, P. St-Jean, M. Milićević, A. Lemaître, A. Harouri, L.L. Gratiet, O. Bleu, D.D. Solnyshkov, G. Malpuech, I. Sagnes, S. Ravets, A. Amo, J. Bloch, *Nat. Photonics* **13**, 283 (2019)
49. N.G. Berloff, M. Silva, K. Kalinin, A. Askitopoulos, J.D. Töpfer, P. Cilibrizzi, W. Langbein, P.G. Lagoudakis, *Nat. Mater.* **16**, 1120 (2017)
50. D. Ballarini, A. Gianfrate, R. Panico, A. Opala, S. Ghosh, L. Dominici, V. Ardizzone, M.D. Giorgi, G. Lerario, G. Gigli, T.C.H. Liew, M. Matuszewski, D. Sanvitto, *Nano Lett.* **20**, 3506 (2020)
51. T. Ozawa, H.M. Price, A. Amo, N. Goldman, M. Hafezi, L. Lu, M.C. Rechtsman, D. Schuster, J. Simon, O. Zilberberg, I. Carusotto, *Rev. Mod. Phys.* **91**, 015006 (2019)
52. X. Xu, H. Xu, S. Mandal, R. Banerjee, S. Ghosh, T.C.H. Liew, *Phys. Rev. B* **103**, 235306 (2021)
53. Y.-M.R. Hu, E.A. Ostrovskaya, E. Estrecho, *Opt. Mater. Express* **14**, 664 (2024)
54. D. Smirnova, D. Leykam, Y. Chong, and Y. Kivshar, *Appl. Phys. Rev.* **7**, 10.1063/1.5142397 (2020)
55. N. Pernet, P. St-Jean, D.D. Solnyshkov, G. Malpuech, N.C. Zambon, Q. Fontaine, B. Real, O. Jamadi, A. Lemaître, M. Morassi, L.L. Gratiet, T. Baptiste, A. Harouri, I. Sagnes, A. Amo, S. Ravets, J. Bloch, *Nat. Phys.* **18**, 678 (2022)
56. C.-E. Bardyn, T. Karzig, G. Refael, T.C.H. Liew, *Phys. Rev. B* **93**, 020502 (2016)
57. H.S. Nguyen, D. Gerace, I. Carusotto, D. Sanvitto, E. Galopin, A. Lemaître, I. Sagnes, J. Bloch, A. Amo, *Phys. Rev. Lett.* **114**, 036402 (2015)
58. K. Falque, Q. Glorieux, E. Giacobino, A. Bramati, and M. J. Jacquet, Spectroscopic measurement of the excitation spectrum on effectively curved spacetimes in a polaritonic fluid of light (2023), arXiv:2311.01392 [cond-mat.quant-gas]

59. D. Gerace, I. Carusotto, *Phys. Rev. B* **86**, 144505 (2012)

60. O. Kyriienko, T.C.H. Liew, I.A. Shelykh, *Phys. Rev. Lett.* **112**, 076402 (2014)

61. J. Restrepo, C. Ciuti, I. Favero, *Phys. Rev. Lett.* **112**, 013601 (2014)

62. A.S. Kuznetsov, D.H.O. Machado, K. Biermann, P.V. Santos, *Phys. Rev. X* **11**, 021020 (2021)

63. N. Carlon Zambon, Z. Denis, R. De Oliveira, S. Ravets, C. Ciuti, I. Favero, and J. Bloch, *Phys. Rev. Lett.* **129**, 093603 (2022)

64. I. Carusotto, D. Gerace, H.E. Tureci, S. De Liberato, C. Ciuti, A. Imamoğlu, *Phys. Rev. Lett.* **103**, 033601 (2009)

65. A. Le Boité, G. Orso, C. Ciuti, *Phys. Rev. Lett.* **110**, 233601 (2013)

66. L. Scarpelli, C. Elouard, M. Johnsson, M. Morassi, A. Lemaitre, I. Carusotto, J. Bloch, S. Ravets, M. Richard, T. Volz, *Nat. Phys.* **20**, 214 (2024)

67. E. Togan, H.-T. Lim, S. Faelt, W. Wegscheider, A. Imamoglu, *Phys. Rev. Lett.* **121**, 227402 (2018)

68. S. Ravets, P. Knüppel, S. Faelt, O. Cotlet, M. Kroner, W. Wegscheider, A. Imamoglu, *Phys. Rev. Lett.* **120**, 057401 (2018)

69. P. Knuppel, S. Ravets, M. Kroner, S. Falt, W. Wegscheider, and A. Imamoglu, *Nature* **572**, 10.1038/s41586-019-1356-3 (2019)

70. R. Shimada, J. Xie, V. Avrutin, U. Ozgur, H. Morkoc, *Appl. Phys. Lett.* **92**, 011127 (2008)

71. T.-C. Lu, Y.-Y. Lai, Y.-P. Lan, S.-W. Huang, J.-R. Chen, Y.-C. Wu, W.-F. Hsieh, H. Deng, *Opt. Express* **20**, 5530 (2012)

72. K. Orfanakis, S.K. Rajendran, V. Walther, T. Volz, T. Pohl, H. Ohadi, *Nat. Mater.* **21**, 767 (2022)

73. C. Klingshirn, *Phys. Status Solidi (b)* **244**, 3027 (2007)

74. C. Klingshirn, R. Hauschild, H. Priller, M. Decker, J. Zeller, and H. Kalt, *Superlattices and Microstructures E-MRS 2005 Symposium G: ZnO and Related Materials*, vol. 38, p. 209 (2005)

75. M. Zamfirescu, A. Kavokin, B. Gil, G. Malpuech, M. Kaliteevski, *Phys. Rev. B* **65**, 161205 (2002)

76. J.-R. Chen, T.-C. Lu, Y.-C. Wu, S.-C. Lin, W.-F. Hsieh, S.-C. Wang, H. Deng, Opt. Express **19**, 4101 (2011)

77. S. Halm, S. Kalusniak, S. Sadofev, H.-J. Wunsche, F. Henneberger, *Appl. Phys. Lett.* **99**, 181121 (2011)

78. S. Kalusniak, S. Sadofev, S. Halm, F. Henneberger, *Appl. Phys. Lett.* **98**, 011101 (2011)

79. F. Li, L. Orosz, O. Kamoun, S. Bouchoule, C. Brimont, P. Disseix, T. Guillet, X. Lafosse, M. Leroux, J. Leymarie, M. Mexis, M. Mihailovic, G. Patriarche, F. Réveret, D. Solnyshkov, J. Zuniga-Perez, G. Malpuech, *Phys. Rev. Lett.* **110**, 196406 (2013)

80. W. Xie, H. Dong, S. Zhang, L. Sun, W. Zhou, Y. Ling, J. Lu, X. Shen, Z. Chen, *Phys. Rev. Lett.* **108**, 166401 (2012)

81. A. Trichet, L. Sun, G. Pavlovic, N. Gippius, G. Malpuech, W. Xie, Z. Chen, M. Richard, L.S. Dang, *Phys. Rev. B* **83**, 041302 (2011)

82. L. Orosz, F. Réveret, F. Médard, P. Disseix, J. Leymarie, M. Mihailovic, D. Solnyshkov, G. Malpuech, J. Zuniga-Pérez, F. Semond, M. Leroux, S. Bouchoule, X. Lafosse, M. Mexis, C. Brimont, T. Guillet, *Phys. Rev. B* **85**, 121201 (2012)

83. A. Trichet, E. Durupt, F. Médard, S. Datta, A. Minguzzi, M. Richard, *Phys. Rev. B* **88**, 121407 (2013)

84. D. Xu, W. Xie, W. Liu, J. Wang, L. Zhang, Y. Wang, S. Zhang, L. Sun, X. Shen, Z. Chen, *Appl. Phys. Lett.* **104**, 082101 (2014)

85. O. Jamadi, F. Reveret, P. Disseix, F. Medard, J. Leymarie, A. Moreau, D. Solnyshkov, C. Deparis, M. Leroux, E. Cambril, S. Bouchoule, J. Zuniga-Perez, and G. Malpuech, *Light* **7**, 82 (2018)

86. L. Zhang, W. Xie, J. Wang, A. Poddubny, J. Lu, Y. Wang, J. Gu, W. Liu, D. Xu, X. Shen, Y.G. Rubo, B.L. Altshuler, A.V. Kavokin, Z. Chen, *Proc. Natl. Acad. Sci.* **112**, E1516 (2015)

87. F. Chen, H. Li, H. Zhou, S. Luo, Z. Sun, Z. Ye, F. Sun, J. Wang, Y. Zheng, X. Chen, H. Xu, H. Xu, T. Byrnes, Z. Chen, J. Wu, *Phys. Rev. Lett.* **129**, 057402 (2022)

88. V. Walther, P. Grunwald, T. Pohl, *Phys. Rev. Lett.* **125**, 173601 (2020)

89. S. A. Lynch, C. Hodges, S. Mandal, W. Langbein, R. P. Singh, L. A. P. Gallagher, J. D. Pritchett, D. Pizzey, J. P. Rogers, C. S. Adams, and M. P. A. Jones, arXiv:2010.11117 [cond-mat, physics:physics] (2020)

90. S. Steinhauer, M.A.M. Versteegh, S. Gyger, A.W. Elshaari, B. Kunert, A. Mysyrowicz, V. Zwiller, *Commun. Mater.* **1**, 1 (2020)

91. J. DeLange, K. Barua, A.S. Paul, H. Ohadi, V. Zwiller, S. Steinhauer, H. Alaeian, *Sci. Rep.* **13**, 16881 (2023)

92. A.S. Paul, S.K. Rajendran, D. Ziemkiewicz, T. Volz, H. Ohadi, *Commun. Mater.* **5**, 43 (2024)

93. K.F. Mak, J. Shan, *Nat. Photonics* **10**, 216 (2016)

94. C. Schneider, M.M. Glazov, T. Korn, S. Höfling, B. Urbaszek, *Nat. Commun.* **9**, 2695 (2018)

95. V. Agranovich, G.C. La Rocca, F. Bassani, H. Benisty, C. Weisbuch, *Opt. Mater.* **9**, 430 (1998)

96. X. Liu, T. Galfsky, Z. Sun, F. Xia, E.-C. Lin, Y.-H. Lee, S. Kéna-Cohen, V.M. Menon, *Nat. Photonics* **9**, 30 (2015)

97. M. Sidler, P. Back, O. Cotlet, A. Srivastava, T. Fink, M. Kroner, E. Demler, A. Imamoglu, *Nat. Phys.* **13**, 255 (2017)

98. F. Barachati, A. Fieramosca, S. Hafezian, J. Gu, B. Chakraborty, D. Ballarini, L. Martinu, V. Menon, D. Sanvitto, S. Kéna-Cohen, *Nat. Nanotechnol.* **13**, 906 (2018)

99. L. Zhang, R. Gogna, W. Burg, E. Tutuc, H. Deng, *Nat. Commun.* **9**, 713 (2018)

100. A. Castellanos-Gomez, M. Buscema, R. Molenaar, V. Singh, L. Janssen, H. S. Van Der Zant, and G. A. Steele, *2D Mater.* **1**, 011002 (2014)

101. B. Munkhbat, P. Wróbel, T.J. Antosiewicz, T.O. Shegai, *ACS Photonics* **9**, 2398 (2022)

102. B. Munkhbat, D.G. Baranov, M. Stuhrenberg, M. Wersall, A. Bisht, T. Shegai, *ACS Photonics* **6**, 139 (2018)

103. R. Bushati, M. Khatoniar, and V. M. Menon, in *CLEO: Applications and Technology* (Optica Publishing Group, 2020) pp. JTh4B–3

104. R. Verre, D.G. Baranov, B. Munkhbat, J. Cuadra, M. Käll, T. Shegai, *Nat. Nanotechnol.* **14**, 679 (2019)

105. H. Zhang, B. Abhiraman, Q. Zhang, J. Miao, K. Jo, S. Roccasecca, M.W. Knight, A.R. Davoyan, D. Jariwala, *Nat. Commun.* **11**, 3552 (2020)

106. N. Muhammad, Y. Chen, C.-W. Qiu, G.P. Wang, *Nano Lett.* **21**, 967 (2021)

107. P.G. Zotev, Y. Wang, D. Andres-Penares, T. Severs-Millard, S. Randerson, X. Hu, L. Sortino, C. Louca, M. Brotons-Gisbert, T. Huq, D.P. Lydzba, D.M. Beggs, D.A. Ritchie, A.I. Tartakovskii, M.S. Skolnick, A.I. Dmitriev, *Laser Photonics Rev.* **17**, 2200957 (2023)

108. X. Xu, W. Yao, D. Xiao, T.F. Heinz, *Nat. Phys.* **10**, 343 (2014)

109. A. Chernikov, T.C. Berkelbach, H.M. Hill, A. Rigosi, Y. Li, B. Aslan, D.R. Reichman, M.S. Hybertsen, T.F. Heinz, *Phys. Rev. Lett.* **113**, 076802 (2014)

110. D. Huang, K. Sampson, Y. Ni, Z. Liu, D. Liang, K. Watanabe, T. Taniguchi, H. Li, E. Martin, J. Levinsen, M.M. Parish, E. Tutuc, D.K. Efimkin, X. Li, *Phys. Rev. X* **13**, 011029 (2023)

111. K.L. Seyler, P. Rivera, H. Yu, N.P. Wilson, E.L. Ray, D.G. Mandrus, J. Yan, W. Yao, X. Xu, *Nature* **567**, 66 (2019)

112. A.K. Geim, I.V. Grigorieva, *Nature* **499**, 419 (2013)

113. N. Peimyoo, T. Deilmann, F. Withers, J. Escolar, D. Nutting, T. Taniguchi, K. Watanabe, A. Taghizadeh, M.F. Craciun, K.S. Thygesen, S. Russo, *Nat. Nanotechnol.* **16**, 888 (2021)

114. W. Liu, Y. Wang, B. Zheng, M. Hwang, Z. Ji, G. Liu, Z. Li, V.J. Sorger, A. Pan, R. Agarwal, *Nano Lett.* **20**, 790 (2019)

115. J. Qin, Y.-H. Chen, Z. Zhang, Y. Zhang, R.J. Blaikie, B. Ding, M. Qiu, *Phys. Rev. Lett.* **124**, 063902 (2020)

116. M. Li, I. Sinev, F. Benimetskiy, T. Ivanova, E. Khestanova, S. Kiriushechkina, A. Vakulenko, S. Guddala, M. Skolnick, V. M. Menon, K. Dmitry, A. Andrea, S. Anton, and K. Alexander, *Nat. Commun.* **12**, 4425 (2021)

117. S. Dufferwiel, T.P. Lyons, D.D. Solnyshkov, A.A. Trichet, F. Withers, S. Schwarz, G. Malpuech, J.M. Smith, K.S. Novoselov, M.S. Skolnick, D.N. Krizhanovskii, A.I. Tartakovskii, *Nat. Photonics* **11**, 497 (2017)

118. Z. Sun, J. Gu, A. Ghazaryan, Z. Shotan, C.R. Considine, M. Dollar, B. Chakraborty, X. Liu, P. Ghaemi, S. Kéna-Cohen, V.M. Menon, *Nat. Photonics* **11**, 491 (2017)

119. N. Lundt, P. Nagler, A. Nalitov, S. Klembt, M. Wurdack, S. Stoll, T. Harder, S. Betzold, V. Baumann, A. Kavokin, C. Schüller, T. Korn, S. Höfling, and C. Schneider, *2D Mater.* **4**, 025096 (2017)

120. S. Dufferwiel, T. Lyons, D. Solnyshkov, A. Trichet, A. Catanzaro, F. Withers, G. Malpuech, J. Smith, K. Novoselov, M. Skolnick, D. Krizhanovskii, A.I. Tartakovskii, *Nat. Commun.* **9**, 4797 (2018)

121. O. Bleu, D. Solnyshkov, G. Malpuech, *Phys. Rev. B* **96**, 165432 (2017)

122. R. Banerjee, S. Mandal, T.C.H. Liew, *Phys. Rev. B* **103**, L201406 (2021)

123. A.M. Jones, H. Yu, N.J. Ghimire, S. Wu, G. Aivazian, J.S. Ross, B. Zhao, J. Yan, D.G. Mandrus, D. Xiao, W. Yao, X. Xu, *Nat. Nanotechnol.* **8**, 634 (2013)

124. N. Lundt, Ł Dusanowski, E. Sedov, P. Stepanov, M.M. Glazov, S. Klembt, M. Klaas, J. Beierlein, Y. Qin, S. Tongay, M. Richard, A.V. Kavokin, S. Höfling, C. Schneider, *Nat. Nanotechnol.* **14**, 770 (2019)

125. I.A. Shelykh, A.V. Kavokin, Y.G. Rubo, T. Liew, G. Malpuech, *Semicond. Sci. Technol.* **25**, 013001 (2009)

126. M. Khatoniar, N. Yama, A. Ghazaryan, S. Guddala, P. Ghaemi, K. Majumdar, V. Menon, *Adv. Opt. Mater.* **11**, 2202631 (2023)

127. C. Rupprecht, E. Sedov, M. Klaas, H. Knopf, M. Blei, N. Lundt, S. Tongay, T. Taniguchi, K. Watanabe, U. Schulz, A. Kavokin, F. Eilenberger, S. Höfling, and C. Schneider, *2D Mater.* **7**, 035025 (2020)

128. S. Dhara, C. Chakraborty, K. Goodfellow, L. Qiu, T. O'Loughlin, G. Wicks, S. Bhattacharjee, A. Vamivakas, *Nat. Phys.* **14**, 130 (2018)

129. B. Chakraborty, J. Gu, Z. Sun, M. Khatoniar, R. Bushati, A.L. Boehmke, R. Koots, V.M. Menon, *Nano Lett.* **18**, 6455 (2018)

130. O. Kyriienko, D. Krizhanovskii, I. Shelykh, *Phys. Rev. Lett.* **125**, 197402 (2020)

131. F. Rana, O. Koksal, M. Jung, G. Shvets, A.N. Vamivakas, C. Manolatou, *Phys. Rev. Lett.* **126**, 127402 (2021)

132. R.P.A. Emmanuele, M. Sich, O. Kyriienko, V. Shahnazaryan, F. Withers, A. Catanzaro, P.M. Walker, F.A. Benimetskiy, M.S. Skolnick, A.I. Tartakovskii, I.A. Shelykh, D.N. Krizhanovskii, *Nat. Commun.* **11**, 3589 (2020)

133. P. Stepanov, A. Vashisht, M. Klaas, N. Lundt, S. Tongay, M. Blei, S. Höfling, T. Volz, A. Minguzzi, J. Renard, C. Schneider, M. Richard, *Phys. Rev. Lett.* **126**, 167401 (2021)

134. J. Gu, V. Walther, L. Waldecker, D. Rhodes, A. Raja, J.C. Hone, T.F. Heinz, S. Kéna-Cohen, T. Pohl, V.M. Menon, *Nat. Commun.* **12**, 2269 (2021)

135. V. Walther, R. Johne, T. Pohl, *Nat. Commun.* **9**, 1309 (2018)

136. L. Zhang, F. Wu, S. Hou, Z. Zhang, Y.-H. Chou, K. Watanabe, T. Taniguchi, S.R. Forrest, H. Deng, *Nature* **591**, 61 (2021)

137. N. Leisgang, S. Shree, I. Paradisanos, L. Sponfeldner, C. Robert, D. Lagarde, A. Balocchi, K. Watanabe, T. Taniguchi, X. Marie, R.J. Warburton, I.C. Gerber, B. Urbaszek, *Nat. Nanotechnol.* **15**, 901 (2020)

138. B. Datta, M. Khatoniar, P. Deshmukh, F. Thouin, R. Bushati, S. De Liberato, S.K. Cohen, V.M. Menon, *Nat. Commun.* **13**, 6341 (2022)

139. C. Anton-Solanas, M. Waldherr, M. Klaas, H. Suchomel, T.H. Harder, H. Cai, E. Sedov, S. Klembt, A.V. Kavokin, S. Tongay, K. Watanabe, T. Taniguchi, S. Höfling, C. Schneider, *Nat. Mater.* **20**, 1233 (2021)

140. J. Zhao, A. Fieramosca, R. Bao, W. Du, K. Dini, R. Su, J. Feng, Y. Luo, D. Sanvitto, T.C.H. Liew, Q. Xiong, *Nat. Nanotechnol.* **17**, 396 (2022)

141. P. Cilibrizzi, X. Liu, P. Zhang, C. Wang, Q. Li, S. Yang, X. Zhang, *Phys. Rev. Lett.* **130**, 036902 (2023)

142. J. Zhao, R. Su, A. Fieramosca, W. Zhao, W. Du, X. Liu, C. Diederichs, D. Sanvitto, T.C. Liew, Q. Xiong, *Nano Lett.* **21**, 3331 (2021)

143. H. Shan, L. Lackner, B. Han, E. Sedov, C. Rupprecht, H. Knopf, F. Eilenberger, J. Beierlein, N. Kunte, M. Esmann, K. Yumigeta, K. Watanabe, T. Taniguchi, S. Klembt, S. Höfling, A.V. Kavokin, S. Tongay, C. Schneider, C. Antón-Solanas, *Nat. Commun.* **12**, 6406 (2021)

144. M. Wurdack, E. Estrecho, S. Todd, C. Schneider, A. Truscott, E. Ostrovskaya, *Phys. Rev. Lett.* **129**, 147402 (2022)

145. S.B. Desai, S.R. Madhvapathy, M. Amani, D. Kiriya, M. Hettick, M. Tosun, Y. Zhou, M. Dubey, J.W. Ager III., D. Chrzan, A. Javey, *Adv. Mater.* **28**, 4053 (2016)

146. B. Lee, W. Liu, C.H. Naylor, J. Park, S.C. Malek, J.S. Berger, A.C. Johnson, R. Agarwal, *Nano Lett.* **17**, 4541 (2017)

147. W. Liu, B. Lee, C.H. Naylor, H.-S. Ee, J. Park, A.C. Johnson, R. Agarwal, *Nano Lett.* **16**, 1262 (2016)

148. W. Liu, Z. Ji, Y. Wang, G. Modi, M. Hwang, B. Zheng, V.J. Sorger, A. Pan, R. Agarwal, *Science* **370**, 600 (2020)

149. F. Dirnberger, R. Bushati, B. Datta, A. Kumar, A.H. MacDonald, E. Baldini, V.M. Menon, *Nat. Nanotechnol.* **17**, 1060 (2022)

150. F. Dirnberger, J. Quan, R. Bushati, G.M. Diederich, M. Florian, J. Klein, K. Mosina, Z. Sofer, X. Xu, A. Kamra, F.J. García-Vidal, A. Alù, V.M. Menon, *Nature* **620**, 533 (2023)

151. J. Wenus, R. Parashkov, S. Ceccarelli, A. Brehier, J.-S. Lauret, M.S. Skolnick, E. Deleporte, D.G. Lidzey, *Phys. Rev. B* **74**, 235212 (2006)

152. H. S. Nguyen, Z. Han, K. Abdel-Baki, X. Lafosse, A. Amo, J.-S. Lauret, E. Deleporte, S. Bouchoule, and J. Bloch, *Appl. Phys. Lett.* **104**, 10.1063/1.4866606 (2014)

153. K. Peng, R. Tao, L. Haeberlé, Q. Li, D. Jin, G.R. Fleming, S. Kéna-Cohen, X. Zhang, W. Bao, *Nat. Commun.* **13**, 7388 (2022)

154. R. Su, J. Wang, J. Zhao, J. Xing, W. Zhao, C. Diederichs, T. C. H. Liew, and Q. Xiong, *Sci. Adv.* **4**, 10.1126/sciadv.aau0244 (2018a)

155. N.H.M. Dang, D. Gerace, E. Drouard, G. Trippé-Allard, F. Lédée, R. Mazurczyk, E. Deleporte, C. Seassal, H.S. Nguyen, *Nano Lett.* **20**, 2113 (2020)

156. N. H. M. Dang, S. Zanotti, E. Drouard, C. Chevalier, G. Trippé-Allard, M. Amara, E. Deleporte, V. Ardizzone, D. Sanvitto, L. C. Andreani, C. Seassal, D. Gerace, and H. S. Nguyen, *Adv. Opt. Mater.* **10**, 10.1002/adom.202102386 (2022)

157. D.B. Mitzi, K. Chondroudis, C.R. Kagan, *IBM J. Res. Dev.* **45**, 29 (2001)

158. J.-C. Blancon, A.V. Stier, H. Tsai, W. Nie, C.C. Stoumpos, B. Traoré, L. Pedesseau, M. Kepenekian, F. Katsutani, G.T. Noe, J. Kono, S. Tretiak, S.A. Crooker, C. Katan, M.G. Kanatzidis, J.J. Crochet, J. Even, A.D. Mohite, *Nat. Commun.* **9**, 2254 (2018)

159. T. Fujita, Y. Sato, T. Kuitani, T. Ishihara, *Phys. Rev. B* **57**, 12428 (1998)

160. A. Brehier, R. Parashkov, J. S. Lauret, and E. Deleporte, *Appl. Phys. Lett.* **89**, 10.1063/1.2369533 (2006)

161. K. Abdel-Baki, F. Boitier, H. Diab, G. Lanty, K. Jemli, F. Lédée, D. Garrot, E. Deleporte, and J. S. Lauret, *J. Appl. Phys.* **119**, 10.1063/1.4941345 (2016)

162. A. Fieramosca, L. Polimeno, V. Ardizzone, L. De Marco, M. Pugliese, V. Maiorano, M. De Giorgi, L. Dominici, G. Gigli, D. Gerace, D. Ballarini, and D. Sanvitto, *Sci. Adv.* **5**, 10.1126/sciadv.aav9967 (2019)

163. L. Polimeno, A. Fieramosca, G. Lerario, M. Cinquino, M. De Giorgi, D. Ballarini, F. Todisco, L. Dominici, V. Ardizzone, M. Pugliese, C. T. Prontera, V. Maiorano, G. Gigli, L. De Marco, and D. Sanvitto, *Adv. Opt. Mater.* **8**, 10.1002/adom.202000176 (2020)

164. R. Su, C. Diederichs, J. Wang, T.C.H. Liew, J. Zhao, S. Liu, W. Xu, Z. Chen, Q. Xiong, *Nano Lett.* **17**, 3982 (2017)

165. R. Su, J. Wang, J. Zhao, J. Xing, W. Zhao, C. Diederichs, T. C. H. Liew, and Q. Xiong, *Sci. Adv.* **4**, 10.1126/sciadv.aau0244 (2018b)

166. J. Wu, S. Ghosh, R. Su, A. Fieramosca, T.C.H. Liew, Q. Xiong, *Nano Lett.* **21**, 3120 (2021)

167. R. Su, S. Ghosh, T. C. H. Liew, and Q. Xiong, *Sci. Adv.* **7**, https://doi.org/10.1126/sciadv.abf8049 (2021b)

168. S. Enomoto, T. Tagami, Y. Ueda, Y. Moriyama, K. Fujiwara, S. Takahashi, and K. Yamashita, *Light* **11**, 8 (2022)

169. P. Bouteyre, H.S. Nguyen, J.-S. Lauret, G. Trippé-Allard, G. Delport, F. Lédée, H. Diab, A. Belarouci, C. Seassal, D. Garrot, F. Bretenaker, E. Deleporte, *ACS Photonics* **6**, 1804 (2019)

170. P. Bouteyre, H. Son Nguyen, J.-S. Lauret, G. Trippé-Allard, G. Delport, F. Lédée, H. Diab, A. Belarouci, C. Seassal, D. Garrot, F. Bretenaker, and E. Deleporte, *Opt. Express* **28**, 39739 (2020)

171. L. Lu, Q. Le-Van, L. Ferrier, E. Drouard, C. Seassal, H.S. Nguyen, *Photonics Res.* **8**, A91 (2020)

172. N. H. M. Dang, P. Bouteyre, G. Trippé-Allard, C. Chevalier, E. Deleporte, E. Drouard, C. Seassal, and H. S. Nguyen, Nanoimprinted exciton-polaritons metasurfaces: Cost-effective, large-scale, high homogeneity, and room temperature operation (2024), arXiv:2403.15956 [physics.optics]

173. M.A. Masharin, V.A. Shahnazaryan, F.A. Benimetskiy, D.N. Krizhanovskii, I.A. Shelykh, I.V. Iorsh, S.V. Makarov, A.K. Samusev, *Nano Lett.* **22**, 9092 (2022)

174. D.G. Lidzey, D.D.C. Bradley, M.S. Skolnick, T. Virgili, S. Walker, D.M. Whittaker, *Nature* **395**, 53 (1998)

175. D.G. Lidzey, D.D.C. Bradley, T. Virgili, A. Armitage, M.S. Skolnick, S. Walker, *Phys. Rev. Lett.* **82**, 3316 (1999)

176. T.K. Hakala, J.J. Toppari, A. Kuzyk, M. Pettersson, H. Tikkanen, H. Kunttu, P. Törma, *Phys. Rev. Lett.* **103**, 053602 (2009)

177. C.P. Dietrich, A. Steude, M. Schubert, J. Ohmer, U. Fischer, S. Höfling, M.C. Gather, *Adv. Opt. Mater.* **5**, 1600659 (2017)

178. R.J. Holmes, S.R. Forrest, *Phys. Rev. Lett.* **93**, 186404 (2004)

179. P. Vasa, W. Wang, R. Pomraenke, M. Lammers, M. Maiuri, C. Manzoni, G. Cerullo, C. Lienau, *Nat. Photonics* **7**, 128 (2013)

180. A. Shalabney, J. George, J. Hutchison, G. Pupillo, C. Genet, T.W. Ebbesen, *Nat. Commun.* **6**, 5981 (2015)

181. S. Kéna-Cohen, S.R. Forrest, *Nat. Photonics* **4**, 371 (2010)

182. K. Georgiou, R. Jayaprakash, A. Othonos, D.G. Lidzey, *Angew. Chem. Int. Ed.* **60**, 16661 (2021)

183. A. Bard, S. Minot, C. Symonds, J. Benoit, A. Gassenq, F. Bessueille, B. Andrioletti, C.R. Pérez de la Vega, K. Chevrier, Y. De Wilde, V. Krachmalnicoff, J. Bellessa, *Adv. Opt. Mater.* **10**, 2200349 (2022)

184. A. Thomas, J. George, A. Shalabney, M. Dryzhakov, S.J. Varma, J. Moran, T. Chervy, X. Zhong, E. Devaux, C. Genet, J.A. Hutchison, T.W. Ebbesen, *Angew. Chem. Int. Ed.* **55**, 11462 (2016)

185. V.M. Agranovich, M. Litinskaia, D.G. Lidzey, *Phys. Rev. B* **67**, 085311 (2003)

186. S. Aberra Guebrou, C. Symonds, E. Homeyer, J. C. Plenet, Y. N. Gartstein, V. M. Agranovich, and J. Bellessa, *Phys. Rev. Lett.* **108**, 066401 (2012)

187. R.T. Grant, P. Michetti, A.J. Musser, P. Gregoire, T. Virgili, E. Vella, M. Cavazzini, K. Georgiou, F. Galeotti, C. Clark, J. Clark, C. Silva, D.G. Lidzey, *Adv. Opt. Mater.* **4**, 1615 (2016)

188. D.M. Coles, P. Michetti, C. Clark, W.C. Tsoi, A.M. Adawi, J. Kim, D.G. Lidzey, *Adv. Func. Mater.* **21**, 3691 (2011)

189. J. Bellessa, C. Bonnand, J.C. Plenet, J. Mugnier, *Phys. Rev. Lett.* **93**, 036404 (2004)

190. P. Törma, W.L. Barnes, *Rep. Prog. Phys.* **78**, 013901 (2015)

191. K. Georgiou, M. Athanasiou, R. Jayaprakash, D.G. Lidzey, G. Itskos, A. Othonos, *J. Chem. Phys.* **159**, 234303 (2023)

192. W. Wang, M. Ramezani, A.I. Vakevainen, P. Törma, J.G. Rivas, T.W. Odom, *Mater. Today* **21**, 303 (2018)

193. A.M. Berghuis, G.W. Castellanos, S. Murai, J.L. Pura, D.R. Abujetas, E. van Heijst, M. Ramezani, J.A. Sánchez-Gil, J.G. Rivas, *Nano Lett.* **23**, 5603 (2023)

194. M. Balasubrahmaniyam, A. Simkhovich, A. Golombek, G. Sandik, G. Ankonina, T. Schwartz, *Nat. Mater.* **22**, 338 (2023)

195. D.G. Lidzey, D.D.C. Bradley, A. Armitage, S. Walker, M.S. Skolnick, *Science* **288**, 1620 (2000)

196. D.M. Coles, N. Somaschi, P. Michetti, C. Clark, P.G. Lagoudakis, P.G. Savvidis, D.G. Lidzey, *Nat. Mater.* **13**, 712 (2014)

197. X. Zhong, T. Chervy, S. Wang, J. George, A. Thomas, J.A. Hutchison, E. Devaux, C. Genet, T.W. Ebbesen, *Angew. Chem. Int. Ed.* **55**, 6202 (2016)

198. K. Chevrier, J. Benoit, C. Symonds, S. Saikin, J. Yuen-Zhou, J. Bellessa, *Phys. Rev. Lett.* **122**, 173902 (2019)

199. K. Daskalakis, S. Maier, S. Kéna-Cohen, *Phys. Rev. Lett.* **115**, 035301 (2015)

200. J. Keeling, S. Kéna-Cohen, *Annu. Rev. Phys. Chem.* **71**, 435 (2020)

201. L. Zhang, J. Hu, J. Wu, R. Su, Z. Chen, Q. Xiong, H. Deng, *Prog. Quantum Electron.* **83**, 100399 (2022)

202. T.K. Hakala, A.J. Moilanen, A.I. Vakevainen, R. Guo, J.-P. Martikainen, K.S. Daskalakis, H.T. Rekola, A. Julku, P. Törma, *Nat. Phys.* **14**, 739 (2018)

203. T. Ishii, K. Miyata, M. Mamada, F. Bencheikh, F. Mathevet, K. Onda, S. Kéna-Cohen, C. Adachi, *Adv. Opt. Mater.* **10**, 2102034 (2022)

204. E. Orgiu, J. George, J.A. Hutchison, E. Devaux, J.F. Dayen, B. Doudin, F. Stellacci, C. Genet, J. Schachenmayer, C. Genes, G. Pupillo, P. Samorì, T.W. Ebbesen, *Nat. Mater.* **14**, 1123 (2015)

205. F. J. Garcia-Vidal, C. Ciuti, and T. W. Ebbesen, *Science* **373**, eabd0336 (2021)

206. J.A. Hutchison, T. Schwartz, C. Genet, E. Devaux, T.W. Ebbesen, *Angew. Chem. Int. Ed.* **51**, 1592 (2012)

207. A. Thomas, L. Lethuillier-Karl, K. Nagarajan, R.M.A. Vergauwe, J. George, T. Chervy, A. Shalabney, E. Devaux, C. Genet, J. Moran, T.W. Ebbesen, *Science* **363**, 615 (2019)
208. A. Mandal, M.A. Taylor, B.M. Weight, E.R. Koessler, X. Li, P. Huo, *Chem. Rev.* **123**, 9786 (2023)

Joel Bellessa is a professor in the Institute of Light and Matter at the University of Lyon, France. His research focuses on the interaction between organic and inorganic semiconductors and metals, and in particular, on plasmon/exciton hybridization and its influence on optical properties (coherence, energy transfer). In addition to organic materials, he is also working on a more applicative subject linked to inorganic semiconductor devices supporting Tamm plasmons. The lasing effect in these low-loss metal/semiconductor systems has been demonstrated and applied to create new light sources such as plasmon generators. Bellessa can reached by email at joel.bellessa@univ-lyon1.fr.

Jacqueline Bloch is a CNRS research director and develops experimental research at the Center for Nanoscience and Nanotechnology, France. She is an expert in semiconductor physics, nonlinear, and quantum optics. Together with her group, she has made groundbreaking contributions to the exploration of quantum fluids of polaritons trapped in lattices of semiconductor microcavities. She was awarded the CNRS Silver Medal, the Jean Ricard prize from the French Physical Society, and the Ampère Prize from the French Academy of Sciences. Since 2019, she has been a Member of the French Academy of Sciences. Bloch can reached by email at jacqueline.bloch@c2n.upsaclay.fr.

Emmanuelle Deleporte was an assistant professor in the Physics Department of Ecole Normale Supérieure Paris, France, from 1992 to 2002, where she gained experience in optical properties of II–VI and III–V inorganic semiconducting heterostructures. In 2002, she moved to Ecole Normale Supérieure Paris-Saclay, France, as a full professor, where she founded her research team about the optical properties of hybrid halide perovskites for applications such as light-emitting devices and photovoltaics. The main topics addressed are related to low-dimensional excitonic effects, carrier relaxation mechanisms, energy and charge transfers, light–matter interaction in cavities. Deleporte can reached by email at emmanuelle.deleporte@ens-paris-saclay.fr.

Vinod Menon is a professor of Physics at the City College of New York and doctoral faculty at the Graduate Center of the City University of New York. He is a Fellow of the Optical Society of America (now Optica), The American Physical Society, and an IEEE Distinguished Lecturer in Photonics (2018–2020). Information about ongoing research in his group can be found at https://lanmp.org/. Menon can reached by email at vmenon@ccny.cuny.edu.

Hai Son Nguyen has been an associate professor at Ecole Centrale de Lyon, France, since 2014, and a junior member of the Institut Universitaire de France since 2020. He holds a physics degree (2009) from École Normale Supérieure de Paris, France, and a PhD degree in physics (2011) with research on single photon emission in semiconductor quantum dots. From 2011 to 2014, he was a CNRS postdoc researcher on photon-exciton coupling. His research at the Institut des Nanotechnologies de Lyon focuses on light–matter interaction in nanophotonics and quantum optics. Nguyen can be reached by email at hai-son.nguyen@ec-lyon.fr.

Hamid Ohadi is a lecturer in physics at the University of St Andrews, Scotland, specializing in photonics and quantum science. His work focuses on light–matter interaction in microcavities and single-particle nonlinearities. He leads the Quantum Light Matter group, exploring strong light–matter interactions in novel materials for quantum technologies. He earned his BSc degree from Sharif University of Technology, Iran, and completed his PhD degree at Imperial College London, where he studied calcium ions in a Penning trap. He has held postdoctoral positions at the University of Southampton and Cambridge, UK, transitioning his research focus toward exciton-polaritons and subsequently, strong light–matter coupling involving Rydberg excitons and two-dimensional materials. Ohadi can be reached by email at ho35@st-andrews.ac.uk.

Sylvain Ravets is a research scientist at the French Centre National de la Recherche Scientifique, France. He works at the Centre de Nanosciences et de Nanotechnologies, located on the Paris-Saclay University campus. His research interests focus on finding new paths to tailor exciton–polaritons in semiconductor microcavities, as a way to investigate topological and quantum physics in engineered polaritonic lattices. He graduated from the École Normale Supérieure de Cachan, France, in 2011. He obtained his PhD degree in 2014, developing novel approaches for quantum engineering using individual atoms. He then turned to exciton polariton systems, working as an ETH postdoctoral fellow in the quantum photonics group at (ETH Zürich). He joined CNRS in 2018 and received an ERC started grant in 2020. Ravets can reached by email at sylvain.ravets@c2n.upsaclay.fr.

Thomas Boulier has been a junior professor Chair since 2022. After obtaining his PhD degree at LKB, France, on exciton–polaritons in 2014, he completed postdoctoral research on cold atoms at NIST, at IOGS, France, with an emphasis on atomic Rydberg states for quantum simulation. In 2020, he was awarded with a junior research chair in the ENS physics department, France, where he developed an original activity on Rydberg states of excitons in the semiconductor copper oxide (Cu_2O). Following his hire as an INSA Jr. Professor, his Rydberg exciton activity moved to LPCNO, Toulouse. Within the Quantum Optoelectronics team, he now focuses on fundamental (giant Kerr effect, excitonic Rydberg interactions, Rydberg states dynamics) and applied (optical quantum sensors) research. Boulier can reached by email at boulier@insa-toulouse.fr.